JACC: BASIC TO TRANSLATIONAL SCIENCE VOL. 7, NO. 8, 2022

ORIGINAL RESEARCH - PRECLINICAL

Iron Overload via Heme Degradation in the Endoplasmic Reticulum Triggers Ferroptosis in Myocardial Ischemia-Reperfusion Injury

Hiroko Deguchi Miyamoto, MD, PhD,[a,b] Masataka Ikeda, MD, PhD,[a,b] Tomomi Ide, MD, PhD,[a,b] Tomonori Tadokoro, MD, PhD,[a,b] Shun Furusawa, MD,[a,b] Ko Abe, MD,[a,b] Kosei Ishimaru, MD,[a,b] Nobuyuki Enzan, MD, PhD,[a,b] Masashi Sada, MD,[a,b] Taishi Yamamoto, MD,[a,b] Shouji Matsushima, MD, PhD,[a,b] Tomoko Koumura, PhD,[c] Ken-ichi Yamada, PhD,[d] Hirotaka Imai, PhD,[c] Hiroyuki Tsutsui, MD, PhD[a,b]

VISUAL ABSTRACT

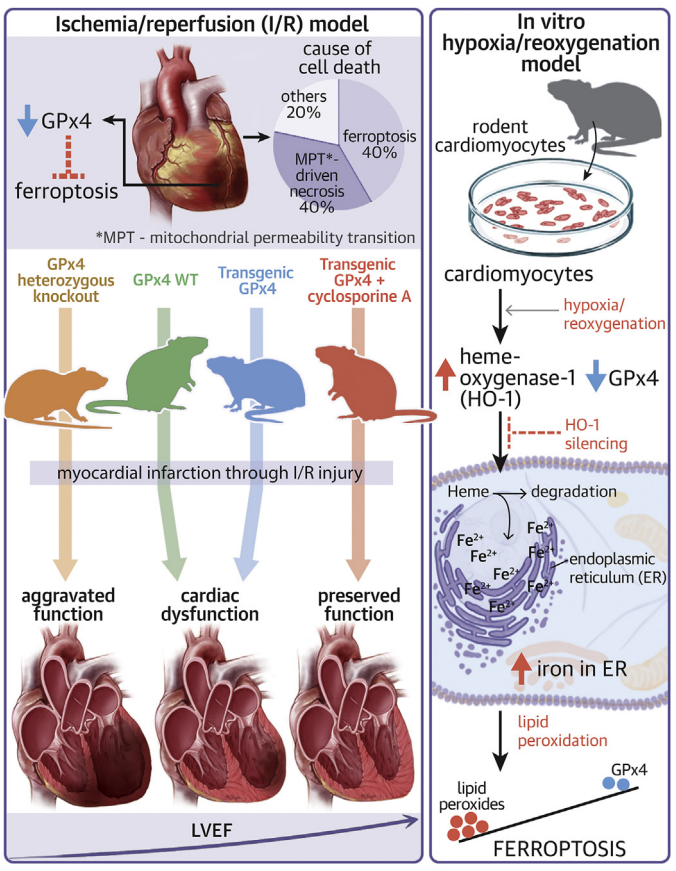

Miyamoto HD, et al. J Am Coll Cardiol Basic Trans Science. 2022;7(8):800-819.

HIGHLIGHTS

- **It remains unknown how ferroptosis, triggered by excessive lipid peroxides via iron overload, is induced in I/R injury.**
- **GPx4, an endogenous suppressor of ferroptosis, is reduced in the myocardium injured by I/R.**
- **Ferroptosis is a major mode of cell death as well as mitochondrial permeability transition-driven necrosis in I/R injury.**
- **Hypoxia-reoxygenation upregulates HO-1, thereby inducing iron overload in the endoplasmic reticulum and ferroptosis in cardiomyocytes.**
- **Therapeutics targeting ferroptosis in conjunction with cyclosporine A can be a promising strategy for I/R injury.**

ISSN 2452-302X https://doi.org/10.1016/j.jacbts.2022.03.012

SUMMARY

Ischemia-reperfusion (I/R) injury is a promising therapeutic target to improve clinical outcomes after acute myocardial infarction. Ferroptosis, triggered by iron overload and excessive lipid peroxides, is reportedly involved in I/R injury. However, its significance and mechanistic basis remain unclear. Here, we show that glutathione peroxidase 4 (GPx4), a key endogenous suppressor of ferroptosis, determines the susceptibility to myocardial I/R injury. Importantly, ferroptosis is a major mode of cell death in I/R injury, distinct from mitochondrial permeability transition (MPT)–driven necrosis. This suggests that the use of therapeutics targeting both modes is an effective strategy to further reduce the infarct size and thereby ameliorate cardiac remodeling after I/R injury. Furthermore, we demonstrate that heme oxygenase 1 up-regulation in response to hypoxia and hypoxia/reoxygenation degrades heme and thereby induces iron overload and ferroptosis in the endoplasmic reticulum (ER) of cardiomyocytes. Collectively, ferroptosis triggered by GPx4 reduction and iron overload in the ER is distinct from MPT-driven necrosis in both in vivo phenotype and in vitro mechanism for I/R injury. The use of therapeutics targeting ferroptosis in conjunction with cyclosporine A can be a promising strategy for I/R injury. (J Am Coll Cardiol Basic Trans Science 2022;7:800–819)

ABBREVIATIONS AND ACRONYMS

AMI = acute myocardial infarction
CsA = cyclosporine A
CypD = cyclophilin D
DXZ = dexrazoxane
ER = endoplasmic reticulum
Fer-1 = ferrostatin-1
GPx4 = glutathione peroxidase 4
HF = heart failure
HO-1 = heme oxygenase 1
H/R = hypoxia-reoxygenation
I/R = ischemia-reperfusion
LP = lipid peroxide
MPT = mitochondrial permeability transition
RCD = regulated cell death
STEMI = ST-segment elevation myocardial infarction

Ischemic heart disease is the leading cause of death worldwide.[1] It culminates in acute myocardial infarction (AMI), a fatal disease accompanied by irreversible myocardial injury. Early reperfusion strategies have been shown to limit the infarct size and markedly improve the outcome of patients with AMI.[2,3] However, as reported by the Framingham Heart Study,[4] the incidence of heart failure (HF) increases after an MI. Therefore, further study is imperative to improve the prognosis of patients after reperfusion therapy in AMI.

Ischemia-reperfusion (I/R) injury has been a promising therapeutic target for patients with AMI since thrombolytic therapy and percutaneous coronary intervention became feasible strategies.[5] Di Lisa et al[6] reported that mitochondrial permeability transition pore (mPTP) opening is a major trigger of cell death in reperfusion injury, and Hausenloy et al[7] demonstrated that cyclosporine A (CsA), an inhibitor of mPTP opening, limits the infarct size in a myocardial I/R model. Mechanistically, cyclophilin D (CypD), which is located in the mitochondria and activated in response to oxidative stress, persistently opens the mPTP, dissipating mitochondrial membrane potential, and finally releases cytochrome c into the cytosol, resulting in mitochondrial permeability transition (MPT)–driven necrosis in reperfusion injury,[8,9] whereas CsA inhibits CypD and thus prevents MPT-driven necrosis.[10] Indeed, in a phase 2 study, CsA reduced the infarct size in patients with ST-segment elevation myocardial infarction (STEMI).[11] However, a phase 3 trial failed to demonstrate the clinical benefit of CsA administration pertaining to clinical outcomes, death from any cause, cardiovascular death, and HF incidence in patients with STEMI.[12] Collectively, these trials suggest that targeting MPT-driven necrosis with CsA therapy is not enough to improve the long-term clinical outcomes. Therefore, additional therapeutic targets for reperfusion injury should be identified.

Ferroptosis is a novel concept of regulated cell death (RCD). Dixon et al[13] first proposed that this RCD mechanism is dependent on iron chelators, and Yang et al[14] showed that glutathione peroxidase 4 (GPx4), a scavenging enzyme for lipid peroxides (LPs), is an endogenous regulator of ferroptosis. Currently, ferroptosis is defined as an RCD initiated by oxidative perturbations of the intracellular

From the [a]Department of Cardiovascular Medicine, Faculty of Medical Sciences, Kyushu University, Fukuoka, Japan; [b]Division of Cardiovascular Medicine, Research Institute of Angiocardiology, Faculty of Medical Sciences, Kyushu University, Fukuoka, Japan; [c]Department of Hygienic Chemistry and Medical Research Laboratories, School of Pharmaceutical Sciences, Kitasato University, Tokyo, Japan; and the [d]Physical Chemistry for Life Science Laboratory, Faculty of Pharmaceutical Sciences, Kyushu University, Fukuoka, Japan.

The authors attest they are in compliance with human studies committees and animal welfare regulations of the authors' institutions and Food and Drug Administration guidelines, including patient consent where appropriate. For more information, visit the Author Center.

Manuscript received February 3, 2022; revised manuscript received March 16, 2022, accepted March 16, 2022.

microenvironment, which is under constitutive control by GPx4 and can be inhibited by iron chelators and lipophilic antioxidants.[10] In this context, Angeli et al[15] reported ferroptosis to be involved in renal I/R injury, and Fang et al[16] demonstrated that treatment with either dexrazoxane (DXZ), an iron chelator, or ferrostatin-1 (Fer-1), a lipophilic antioxidant, reduces the infarct size in myocardial I/R injury. However, it is unclear whether therapeutics targeting ferroptosis in conjunction with CsA can potentiate cardioprotection against I/R injury. In addition, the molecular basis for susceptibility to ferroptosis in myocardial I/R injury remains to be fully elucidated.

Gpx4 is a unique gene that encodes 3 isoforms: cytosolic, mitochondrial, and nucleolar GPx4.[17] Cytosolic GPx4 is a scavenger of lipid peroxides in the phospholipid bilayer of various intracellular organelles, whereas mitochondrial GPx4, with a mitochondrial signaling peptide, is located only in the mitochondria. Using *Gpx4* gene-manipulated mice and adenoviruses harboring cytosolic and mitochondrial *Gpx4* (Ad-cytoGPx4 and Ad-mitoGPx4, respectively), we recently identified the mitochondria as a pivotal organelle involved in doxorubicin-induced ferroptosis in its cardiotoxicity.[18] This suggested that these mice and adenoviruses are effective modalities for investigating the role of ferroptosis in myocardial I/R injury.

In the present study, we investigated the role of GPx4 in ferroptosis-induced myocardial I/R injury and analyzed whether ferroptosis can be a major therapeutic target independently from MPT-driven necrosis by the use of Gpx4 gene-manipulated mice. Furthermore, we investigated the mechanisms underlying the susceptibility of cardiomyocytes to ferroptosis induced by hypoxia-reoxygenation (H/R) by the use of adenoviruses harboring cytosolic and mitochondrial *Gpx4* along with organelle-specific iron chelators.

METHODS

ANIMAL STUDY. All procedures involving animals and animal care protocols were approved by the Committee on Ethics of Animal Experiments at the Kyushu University Faculty of Medical and Pharmaceutical Sciences and performed in accordance with the Guidelines for Animal Experiments of Kyushu University (A20-320), as well as the Guideline for the Care and Use of Laboratory Animals published by the United States National Institutes of Health (NIH) (8th edition, revised in 2011). C57BL/6J mice and Sprague-Dawley rats (CLEA Japan) were housed in a temperature- and humidity-controlled room, fed a commercial diet (CRF-1, Oriental Yeast), and given free access to water. GPx4-transgenic (Tg) (Fγ line) and GPx4-knockout in C57BL/6J mice were induced as described previously.[18-22]

MURINE MYOCARDIAL I/R MODEL. The murine myocardial I/R model was produced as described previously.[23,24] Briefly, 9-12-week-old male mice were anesthetized with 1%-2% isoflurane with the use of an inhalation anesthesia apparatus (MK-AT210D, Muromachi Kikai), the intercostal space was opened under mechanical ventilation, and myocardial ischemia was induced by ligation of the left anterior descending coronary artery (LAD) for 30 minutes followed by reperfusion. The LAD of animals in the sham group was sutured without ligation. CsA (2.5 mg/kg diluted with saline solution to 7.5 mg/mL, 3999406A1032, Novartis International) was injected via the femoral vein 10 minutes before reperfusion. When the mice demonstrated decreased activity after the operation, they were administered carprofen (4.4 mg/kg subcutaneously). After death by intraperitoneal administration of an overdose of a mixture comprising medetomidine (1.5 mg/kg), midazolam (20 mg/kg), and butorphanol tartrate (25 mg/kg) (Wako Chemicals), hearts were excised for either measurement of infarct size 24 hours after reperfusion or Western blot and real-time polymerase chain reaction (PCR) analysis 6, 15, 24, 48, and 72 hours after reperfusion.

ECHOCARDIOGRAPHY. Echocardiographic data were measured through 2-dimensional targeted M-mode images in the short-axis view at the papillary muscle level with the use of a Vevo1100 ultrasonography system (Fujifilm Visual Sonics), as described previously.[18]

ACROLEIN STAINING OF THE MYOCARDIUM EX VIVO. The acrolein was fluor-stained in the myocardium with the use of AcroleinRED (FDV-0022, Funakoshi).[25] Briefly, the heart was rapidly excised 24 hours after reperfusion and cut at the middle and apex levels. The pieces were incubated in a solution containing AcroleinRED (20 μmol/L) and Hoechst 33342 (5 μg/mL, H3570, Thermo Fisher Scientific) for 15 minutes at room temperature. After washing with phosphate-buffered saline solution (PBS), the sections on slide glass were observed with the use of a fluorescence microscope (BZ-X800, Keyence).

ASSESSMENT OF MYOCARDIAL INFARCT SIZE. The Evans Blue–triphenyltetrazolium chloride (TTC) double-staining method was used to determine myocardial infarct size as described previously.[23,24] The LAD was reoccluded and 0.3 mL 2% Evans Blue dye was injected into the right jugular vein to identify the area at risk (AAR) 24 hours after reperfusion. Once

the peripheral limbs turned blue, the heart was rapidly excised and rinsed in normal saline solution, and the left ventricle (LV) was frozen in liquid nitrogen. The LV was then cut into 5 1-mm-thick slices, which were incubated in 1% 2,3,5-TTC (T0520, Tokyo Chemical Industry) for 15 minutes at 37 °C. The infarct area (IFA) (white) and the AAR (red and white) for each segment were measured with the use of ImageJ v1.44 (NIH). Thereafter, the AAR/LV, IFA/AAR, and IFA/LV ratios were calculated.

PLASMA TROPONIN I MEASUREMENT. Whole blood was collected 24 hours after reperfusion, and plasma was isolated by centrifugation at 13,200 rpm for 10 minutes. Plasma troponin I levels were measured with the use of an enzyme-linked immunosorbent assay kit (CTNI-1-HSP, Life Diagnostics).

TERMINAL DEOXYNUCLEOTIDYL TRANSFERASE–MEDIATED dUTP NICK-END LABELING. Terminal deoxynucleotide transferase-mediated dUTP nick-end labeling (TUNEL) staining was performed to detect in situ DNA fragmentation with the use of an apoptosis detection kit (MK500, Takara) as described previously.[26,27] Briefly, hearts were retrieved 24 hours after reperfusion and stored in 10% formalin. Then, they were cut on the short axis into 3 sections: base, middle, and apex. Each section was embedded in paraffin, cut into 3-mm slices, and stained according to the manufacturer's instructions. Briefly, the sliced samples were deparaffinized and washed with PBS. The deparaffinized samples were processed with proteinase K (20 μg/mL, 161-28701, Fujifilm Wako Pure Chemical Corp) for 15 minutes and washed with PBS 3 times. The samples were then labeled with antibody against cardiac troponin T (ab209813, Abcam) and placed in an incubator at 37 °C for 60 minutes. After the samples were washed with PBS, fragmented DNA was labeled in Labeling Safe Buffer with terminal deoxynucleotide transferase, and the samples were treated with the secondary antibody (DI-1594, Vector Laboratories) at 37 °C in an incubator for 90 minutes. The samples were washed with PBS and sealed with mounting agent (Vectashield H1800, Vector Laboratories). The samples were observed under a fluorescence microscope (BZ-X800, Keyence), and TUNEL-positive and cardiac troponin T-positive cells were counted as TUNEL-positive cardiomyocytes.

REAGENTS. Fer-1 (SML0583) was purchased from Sigma-Aldrich. DXZ (ab141109) was purchased from Abcam. FerroOrange (F374) and Mito-FerroGreen (MFG, M489) were purchased from Dojindo. Ferro-FarRed (FFR, GC903-01) was purchased from Goryo Chemical. CsA (C2408) was purchased from Tokyo Chemical Industry.

CELL CULTURE. Primary cultures of the isolated neonatal rat ventricular cardiomyocytes were prepared from the ventricles of neonatal Sprague-Dawley rats as described previously.[18,23] Neonatal rats were killed by administering an overdose of isoflurane (5%), and the hearts were then rapidly excised. After digesting the myocardial tissues with trypsin (25300-062, Thermo Fisher Scientific) and collagenase type 2 (LS004176, Worthington Biochemical), the isolated cardiomyocytes were suspended in DMEM (D5796, Sigma-Aldrich) containing 10% fetal bovine serum (SH30910.03, HyClone Laboratories) and 1% penicillin/streptomycin (26253-84, Nacalai Tesque). Cells were plated twice in 100-mm culture dishes for 70 minutes each to reduce the number of non-myocytes. Nonadherent cells were plated in culture dishes (Primaria, Corning) at $\sim 2.5 \times 10^5$/mL for each experiment as cultured cardiomyocytes and maintained at 37 °C in humidified air with 5% CO_2.

H/R IN CULTURED CARDIOMYOCYTES. Cultured cardiomyocytes were perturbated by H/R as described previously with some modifications.[23] Briefly, hypoxia (Hx) was induced by replacing the standard medium with a conditioned medium that was kept in a hypoxic chamber (APM-50D, Astec) overnight (5%~ CO_2, 94.5% N_2, 0.5% O_2 at 37 °C), and then the cultured cardiomyocytes were incubated in the hypoxic chamber for 24 hours. Reoxygenation was induced by reincubating them under standard conditions. Fer-1 (50 μmol/L), DXZ (1 mmol/L), CsA (2 μM→μmol/L), MFG (10 μmol/L), and FFR (10 μmol/L) were added 1 hour before inducing H/R.

ISOLATION OF ADULT MOUSE CARDIOMYOCYTES. Adult mouse cardiomyocytes were isolated as described previously,[28] with some modifications. Briefly, 5-6-week-old male mice were anesthetized with 1%-4% isoflurane under mechanical ventilation using an inhalation anesthesia apparatus with oxygen (flow rate; 0.5 L/min). The heart of the mice was exposed at the thoracic diaphragm, and 7 mL of EDTA buffer was injected at the mid portion of right ventricle within 1 min. After clamping the ascending aorta, the heart was excised onto a 60-mm Petri dish filled with EDTA buffer. Subsequently, 10 mL of EDTA buffer was injected at the apex at the rate of 1 mL per 2-3 min. The heart samples were then transferred to a Petri dish filled with perfusion buffer, and 3 mL of perfusion buffer was subsequently injected via the same needle hole at the apex. Thereafter, the heart was transferred to a Petri dish filled with collagenase buffer, and approximately 25 mL of collagenase buffer was injected until characteristics of degradation were observed. Subsequently, clamping was

removed, and the left ventricle was isolated. The left ventricle was cut into 1-mm^2 pieces in 3 mL collagenase buffer, and the tissue was loosened by pipetting for 2 minutes. Stop buffer (5 mL) was added to the suspended solution in collagenase buffer, and the mixture was pipetted for 2 minutes. Undegraded tissues were removed by passing the suspension through a filter (pore size 100 μm, 352360, Corning). Adult cardiomyocytes were allowed to settle by keeping the suspension still. To neutralize the adult cardiomyocytes to M199-based culture medium, the pellet was subsequently suspended in mixed buffers (calcium reintroduction buffers) of perfusion buffer and culture medium at, respectively, 2:1, 1:1, and 1:2. The pellet was finally suspended in plating medium, and adult cardiomyocytes were plated at 1,500 cells per well in a 96-well plate for a cell survival assay and the 1,000 cells per well in a 35-mm dish for iron measurement using FFR (the plates were coated with 5 μg/mL laminin [23017015, Thermo Fisher Scientific] solution). The plating medium was changed to culture medium with 5% fetal bovine serum (Hyclone) 1 hour after incubation. The compositions of EDTA buffer, perfusion buffer, collagenase buffer, stop buffer, plating medium, and culture medium were the same as those described previously.[28] Hx and H/R were induced as described in neonatal culture cardiomyocytes, although the durations of Hx and reoxygenation were 12 and 6 hours, respectively. Fer-1 and CsA were used at 50 μmol/L and 2 μmol/L, respectively.

ADENOVIRUS CONSTRUCTION. Ad-cytoGPx4 and Ad-mitoGPx4 were produced as described previously.[18] Cultured cardiomyocytes were infected with these adenoviruses for 1 hour, followed by incubation for 48 hours in standard medium, and then used in subsequent experiments.

TRANSFECTION OF SMALL INTERFERING RNA. Silencing of heme oxygenase 1 (*Hmox1*) (5 nmol/L, s127884, Thermo Fisher Scientific), transferrin receptor (*Tfrc*) (10 nmol/L, s134442, Thermo Fisher Scientific), and ferroportin (*Slc40a1*) (10 nmol/L, s139390, Thermo Fisher Scientific) was performed by small interfering RNA (siRNA) transfection with Lipofectamine RNAiMAX (Thermo Fisher Scientific) according to the manufacturer's instructions. Briefly, 24 hours after seeding, the cardiomyocytes were transfected with siRNA and incubated for 48 hours.

WESTERN BLOTTING. Western blotting was performed as previously described.[29,30] Primary antibodies against the following proteins were used: GPx4 (ab125066, Abcam), acrolein (MAR-020n, JaICA; Shizuoka), and heme oxygenase-1 (HO-1) (43966, CST). Coomassie blue staining (11642-31, Nacalai Tesque) was used to standardize the signal intensity detected by Western blotting.

QUANTITATIVE REVERSE-TRANSCRIPTION PCR. Total RNA extraction and quantitative reverse-transcription PCR were performed as described previously,[31,32] with some modifications. Briefly, total RNA was extracted with the use of an RNeasy Mini Kit (74104, Qiagen) and converted to cDNA with the use of ReverTra Ace qPCR RT Kit (FSQ-201, Toyobo), and the reactions were run in an Applied Biosystems QuantStudio3 (Thermo Fisher Scientific) for the Thunderbird SYBR qPCR Mix (Toyobo). Relative gene expression was normalized by the expression of an internal control gene (*Rps18*). The forward (F) and reverse (R) primer sequences, respectively, were as follows: *Rps18* (mouse): F 5′-TTCTGGCCAACGGTCTAGACAAC-3′, R 5′-CCAGTGGTCTTGGTGTGCTGA-3′; total *Gpx4* (mouse): F 5′-CGCGATGATTGGCGCT-3′, R 5′-CACACGAAACCCCTGTACTTATCC-3′; mitochondrial *Gpx4* (mouse): F 5′-AGCTGGGGCCGTCTGAGCCG-3′, R 5′-ATGTCCTTGGCTGAGAATTCGT-3′; nucleolar *Gpx4* (mouse): F 5′-CTGAACCTTTCAACCCGGG-3′, R 5′-AGAATTCGTGCATGGAGCG-3′; *Rps18* (rat): F 5′-AAGTTTCAGCACATCCTGCGAGTA-3′, R 5′-TTGGTGAGGTCAATGTCTGCTTTC-3′; total *Gpx4* (rat): F 5′-TCAATGTCTGCTTTC-3′; mitochondrial *Gpx4* (rat): F 5′-CGCTTATTGAAGCCAGCACT-3′, R 5′-TTATCCAGGCAAACCATGTG-3′; nucleolar *Gpx4* (rat): F 5′-TCTGCTGCAGGACCTTCC-3′, R 5′-CGCAACCCCTGTACTTATCC-3′; *Hmox1* (rat): F 5′-AGGTGCACATCCGTGCAGAG-3′, R 5′-CTTCCAGGGCCGTATAGATATGGTA-3′; *Tfrc* (rat): F 5′-GGATCAAGCCAGATCAGCAT-3′, R 5′-CTCATCTGCAGCCAGTTTCA-3′; *Slc40a1* (rat): F 5′-ACAGCTGTCTACGGGTTGGT-3′, R 5′-ATGATCCCGCAGAGAATGAC-3′.

COMPLEX I ACTIVITY. Complex I activity was measured with the use of a Complex I Enzyme Activity Assay Kit (ab109721, Abcam). Briefly, ∼10 mg of myocardium was homogenized in PBS, and sample A (5.5 mg/mL) was prepared by adding PBS to each extract. Detergent solution (10 μL) was added to sample A, and the mixture kept on ice for 30 minutes. Subsequently, the mixture was centrifuged at 16,000*g* for 20 minutes at 4 °C and the supernate collected as sample B. Sample B was diluted with incubation solution (1:20 ratio of sample B to incubation solution). Diluted sample B (200 μL) was added onto a 96-well plate and kept at room temperature for 3 hours. Thereafter, the diluted solution was fully removed from the 96-well plate, and each well was washed with 1× wash buffer 3 times. Finally, assay solution was added to each well and

the absorbance was repeatedly measured at 450 nm at 30-second intervals for 30 minutes at 30 °C. Complex I activity was defined by the rate of change in optical density (OD) per minute ([absorbance2 – absorbance1]/time).

COMPLEX IV ACTIVITY. Complex IV activity was measured with the use of a Complex IV Rodent Enzyme Activity Microplate Assay Kit (ab109911, Abcam). Briefly, ~10 mg of myocardium was homogenized in solution 1, and sample A (5.5 mg/mL) was prepared by adding solution 1 to each extract. Detergent solution (10 μL) was added to sample A, and the mixture were kept on ice for 30 minutes. Subsequently, the mixture was centrifuged at 16,000*g* for 20 minutes at 4 °C and the supernate collected as sample B. Sample B was diluted with solution 1 (1:20 ratio of sample B to solution 1). Diluted sample B (200 μL) was added into a 96-well plate and kept at room temperature for 3 hours. Thereafter, the diluted solution was fully removed from the 96-well plate, and each well was washed with solution 1 three times. Finally, assay solution (200 μL, reagent C plus solution 1) was added into each well, and the absorbance was repeatedly measured at 550 nm at 1-minute intervals for 120 minutes at 30 °C. Complex IV activity was defined by the rate of change in OD per minutes ([absorbance2 – absorbance1]/time).

CELL SURVIVAL ASSAY USING CALCEIN ACETOXYMETHYL (AM). To assess cell viability, the calcein assay was performed with neonatal rat cardiomyocytes and adult mouse cardiomyocytes that were seeded in 96-well (1 × 8 Stripwell; 9102, Life Sciences) after H/R (24 h Hx and 24 h reoxygenation in neonatal rat cardiomyocytes and 12 h Hx and 6 h reoxygenation in adult mouse cardiomyocytes), with the use of Cell Counting Kit F (CK-06, Dojindo) as described previously.[18,23] Briefly, after being washed with PBS, cultured cells were incubated in calcein AM solution diluted in PBS (1:500 ratio of calcein AM to PBS) for 15 minutes at 37 °C. Thereafter, cell viability was fluorometrically measured (excitation wavelength of 490 nm and emission wavelength of 520 nm) with the use of a Varioskan LUX Multimode Microplate Reader (Thermo Fisher Scientific).

EXTRACTION OF ENDOPLASMIC RETICULUM FROM MYOCARDIUM. Endoplasmic reticulum (ER) was extracted from the myocardium with the use of an Endoplasmic Reticulum Enrichment Extraction Kit (NBP2-29482, Novus Biologicals). Briefly, frozen myocardium (~50 mg) was first washed in 1 mL PBS. Subsequently, myocardium was homogenized in isosmotic homogenization buffer (4 μL/mg) containing 100× protease inhibitor cocktail (0.04 μL/mg). The homogenates were transferred to a centrifuge tube and centrifuged at 1,000*g* for 10 minutes at 4 °C. The supernates were transferred to clean tubes and centrifuged at 12,000*g* for 15 minutes at 4 °C. Thereafter, the supernates were transferred to new tubes and centrifuged at 90,000*g* for 60 minutes at 4°C. Pellets were suspended with isosmotic homogenization buffer (7 μL/mg), and the suspensions were used for iron measurement.

IRON MEASUREMENT USING THE FERROZINE METHOD. Iron contents in cell lysate and ER extract lysate were measured with the use of a Metallo Assay Kit (FE31M, Metallogenics) based on the ferrozine method as described previously.[18] Briefly, 6 mol/L HCl was added to 55 μL lysate, and the mixture was placed for 30 minutes at room temperature. Afterward, the mixtures were spun down to obtain the supernate. The supernates (40 μL) were mixed with R-A buffer (200 μL) on a 96-well plate. After 5 minutes of reactions, the base line absorbance of the samples was measured at 560 nm (OD1) with the use of a Varioskan LUX Multimode Microplate Reader (Thermo Fisher Scientific). Subsequently, R-R Chelator-Color (8 μL) was added to the samples, and the absorbance was measured again at 560 nm (OD2). The increase in absorbance, ie, OD2 – OD1, was calculated, and iron content was determined based on a standard curve.

MEASUREMENTS OF LIPID PEROXIDATION WITH THE USE OF C11-BODIPY 581/591. LPs were measured with the use of C11-BODIPY 581/591 (Thermo Fisher Scientific) in cultured cardiomyocytes after 24 hours Hx and 1 hour reoxygenation. The cells were harvested by trypsinization and resuspended with PBS. Then, the cells were incubated with PBS containing C11-BODIPY 581/591 (2 μmol/L) for 15 minutes at 37 °C. They were strained through a 40-μm cell strainer (pluriSelect 43-10040, Life Science), and analyzed with the use of a flow cytometer (BD FACSLyric, BD Biosciences) equipped with a 488 nm laser for excitation. At least 10,000 cells were analyzed per condition. The data were presented with the use of FlowJo v10.

FLUORESCENCE IMAGING FOR FERROUS IRON. FerroOrange and FFR were used to detect ferrous iron (Fe^{2+}) in whole cells and ER, respectively. Cultured cardiomyocytes were seeded on a 35-mm glass-bottomed dish (AGC Techno Glass) and washed 3 times with PBS, and the medium was replaced with fresh DMEM without serum containing 1 μmol/L

FerroOrange or 5 μmol/L FFR and 0.1 μmol/L ERseeing (FDV-0038; Funakoshi), in the presence or absence of 1 mmol/L DXZ. Hx was induced using conditioned media from the hypoxic chamber, followed by incubating the cells in the hypoxic chamber for 4 h. Afterwards, the cells were washed thrice with PBS and fixed with 4% paraformaldehyde for 10 minutes at 4 °C. After being washed 3 times with PBS, they were mounted on a microscopic slide with the use of a mounting medium with 4',6-diamidino-2-phenylindole (DAPI) (Vectashield H1200, Vector Laboratories) and observed under a fluorescence microscope (BZ-X800, Keyence). Image analysis was performed with the use of ImageJ v1.44.

MEMBRANE POTENTIAL IN CARDIOMYOCYTES. Membrane potential was assessed with the use of the MitoProbe JC-1 assay (M34152, Thermo Fisher Scientific) in accordance with the manufacturer's instructions. Briefly, the isolated cardiomyocytes were washed with PBS and treated with 2 μmol/L JC-1 at 37 °C for 15 minutes. After the cardiomyocytes were washed with PBS, they were collected on ice with the use of a scraper in cold PBS and centrifuged at 1,000 rpm for 5 minutes at 4 °C. The pellet was resuspended by tapping in 250 μL PBS, and aggregates were removed by passing the suspension through a filter (pluriSelect 43-10040, Life Science). The cardiomyocytes were analyzed with the use of a flow cytometer (BD FACSLyric). The fluorescence intensity of PE was assessed as membrane potential. Positive control was prepared by treating the cardiomyocytes with 200 μmol/L protonophore m-chlorophenylhydrazone at 37 °C for 60 minutes.

STATISTICAL ANALYSIS. Data are presented as mean ± SEM. Data were evaluated for departures from the normal distribution. Two groups were compared with the use of Student's *t*-test, and 3 or more groups were compared with the use of 1-way analysis of variance with Tukey's honest significance difference test for multiple pairwise comparisons. Dunnett's test was used to control type I error when comparing multiple groups with the control (e.g., sham). A P value of <0.05 was considered to be statistically significant, with $^{*}P < 0.05$, $^{**}P < 0.01$, and $^{***}P < 0.001$ indicating significance within the figures. JMP v15 (SAS Institute) was used for all statistical analyses.

RESULTS

MYOCARDIAL I/R INJURY REDUCED GPx4 AND INCREASED LP LEVELS. The I/R model in the present study showed ~40% infarct area (IFA) per area-at risk (IFA/AAR) at 24 hours (Supplemental Figures 1A and 1B) and impairment of left ventricular ejection fraction (LVEF) and cardiac dilation on day 14 after I/R (Supplemental Figures 1C and 1D). The expression of all isoforms of *Gpx4* was significantly down-regulated (**Figure 1A**), and the acrolein level, representing LPs, was elevated in the I/R-injured myocardium 24 hours after reperfusion (**Figure 1B**). The Western blot analysis showed that the GPx4 level was reduced and the acrolein level was increased in the I/R-injured myocardium (**Figure 1C**). GPx4 levels continued to decrease until 48 hours, and then recovered to those of the sham mice 72 hours after reperfusion (**Figure 1C**). In contrast, acrolein levels were increased in the I/R-injured myocardium 24 hours after reperfusion, with further gradual increase until 72 hours after reperfusion (**Figure 1C**), although the activities of complex I and IV, representing mitochondrial function, were not suppressed in the I/R injured myocardium (Supplemental Figure 2). The number of TUNEL-positive cells, which have previously been observed during ferroptosis,[18,33] increased in the I/R-injured myocardium (**Figure 1D**). These results suggest that a reduction in GPx4 levels enhances the susceptibility of the I/R-injured myocardium to ferroptosis, as well as indicate the involvement of ferroptosis in myocardial I/R injury.

OVEREXPRESSION OF GPx4 ATTENUATED MYOCARDIAL I/R INJURY. To investigate the roles of GPx4 and ferroptosis in myocardial I/R injury, we used GPx4 Tg mice, in which the DNA sequence of *Gpx4* with endogenous promoter was inserted, and all *Gpx4* isoforms were globally overexpressed.[20,21] The overexpression of GPx4 significantly reduced the IFA/AAR ratio 24 hours after reperfusion compared with that of wild-type (WT) mice (**Figure 2A**). Consistently, plasma troponin I levels were significantly lower in GPx4 Tg mice than in WT mice (**Figure 2B**). GPx4 overexpression attenuated the increase in acrolein levels in the I/R-injured myocardium (**Figure 2C**). The number of TUNEL-positive cells was reduced in GPx4 Tg mice (**Figure 2D**). Given that GPx4 is a specific endogenous regulator of ferroptosis, the reduced number of TUNEL-positive cells by the overexpression of GPx4 indicates that cells died due to ferroptosis.

HETERO-DELETION OF GPx4 AGGRAVATED MYOCARDIAL I/R INJURY. GPx4 hetero-knockout (hetKO) mice had a higher IFA/AAR ratio 24 hours after reperfusion than WT mice (**Figure 3A**). Plasma troponin I levels were higher in hetKO mice than in WT mice (**Figure 3B**). GPx4 levels were significantly lower in hetKO mice than in WT mice, and acrolein levels were significantly enhanced in hetKO mice (**Figure 3C**). The number of TUNEL-positive cells was higher in the I/R-injured myocardium of hetKO mice

FIGURE 1 Myocardial I/R Injury Decreased GPx4 and Increased Lipid Peroxide Levels

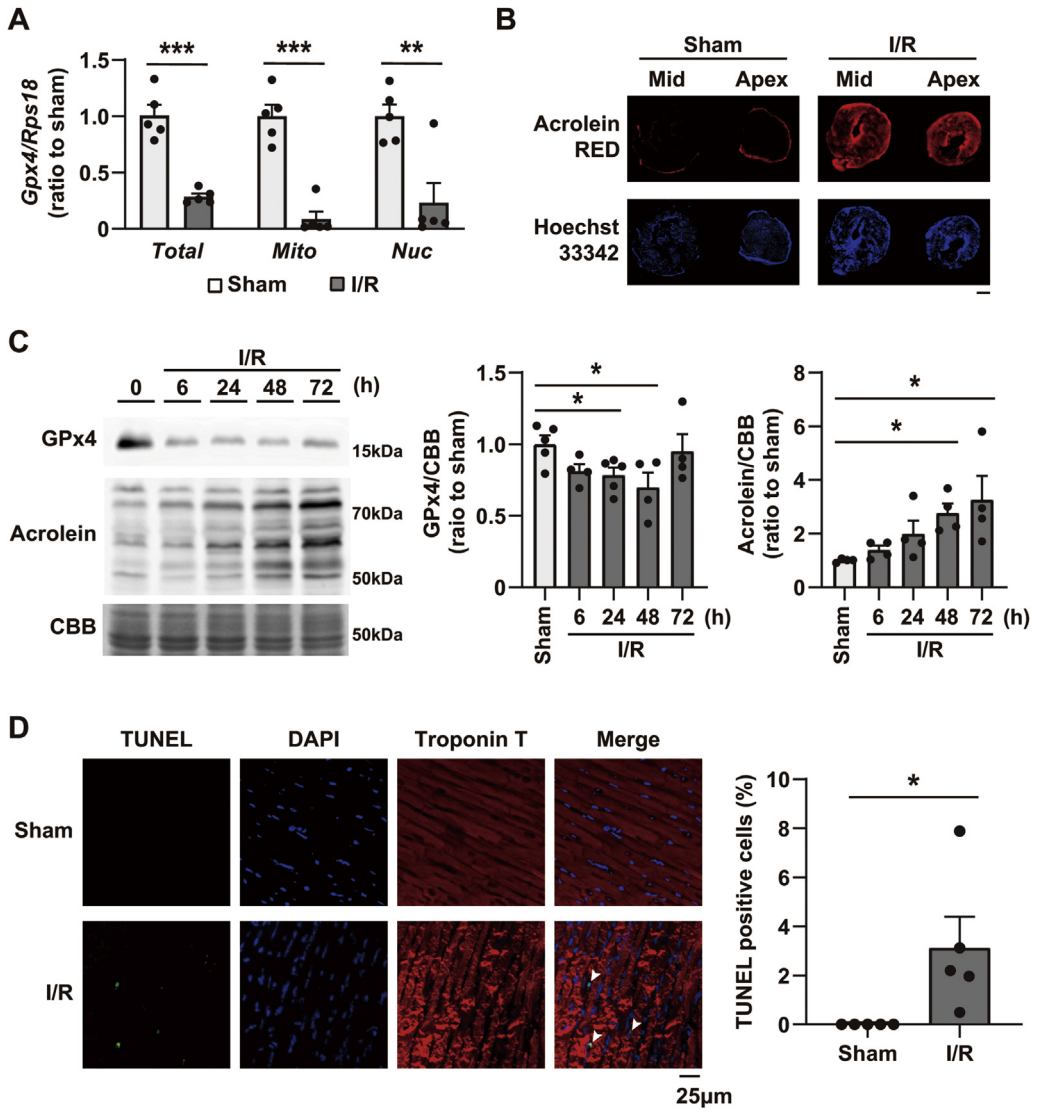

(A) Expression of total, mitochondrial (Mito), and nucleolar (Nuc) Gpx4 in the I/R-injured myocardium 24 hours after reperfusion was quantified by quantitative real-time polymerase chain reaction (n = 5). **(B)** Acrolein staining with the use of AcroleinRED **(red)** and Hoechst 33342 **(blue)** in the myocardium injured by I/R. Scale bar = 1 mm. **(C) (left)** Western blot of GPx4 and acrolein levels in the area at risk of respective hearts 6, 24, 48, and 72 hours after reperfusion; **(right)** quantification of Western blot results (n = 4-5). Each band intensity was standardized to Coomassie Brilliant Blue (CBB) staining (50 kDa). **(D) (left)** Representative images of TUNEL staining **(green)** and co-staining with DAPI **(blue)** and troponin T **(red)**, and **(right)** the number of TUNEL and DAPI double-positive nuclei in troponin T-positive myocardium 24 hours after →reperfusion (n = 5). Scale bar = 25 μm; **arrowheads** indicate TUNEL-positive nuclei. Data are shown as mean ± SEM. Statistical significance was determined by means of **(A and D)** Student's *t*-test and **(C)** Dunnett's test (vs sham). *$P < 0.05$, **$P < 0.01$, ***$P < 0.001$. DAPI = 4',6-diamidino-2-phenylindole; Gpx4 = glutathione peroxidase 4; I/R = ischemia-reperfusion; TUNEL = terminal deoxynucleotidyl transferase–mediated dUTP nick-end labeling

than in WT mice (Figure 3D). Collectively, these results suggest that GPx4-regulated ferroptosis is responsible for myocardial I/R injury, and that GPx4 determines the susceptibility to ferroptosis in myocardial I/R injury.

FERROPTOSIS WAS DISTINCT FROM MPT-DRIVEN NECROSIS IN MYOCARDIAL I/R INJURY. In myocardial I/R injury, MPT-driven necrosis is a major mode of cell death.[6,7] Oxidative stress triggers the opening of mPTP, thereby disrupting the mitochondrial

FIGURE 2 GPx4 Overexpression Ameliorated Myocardial I/R Injury

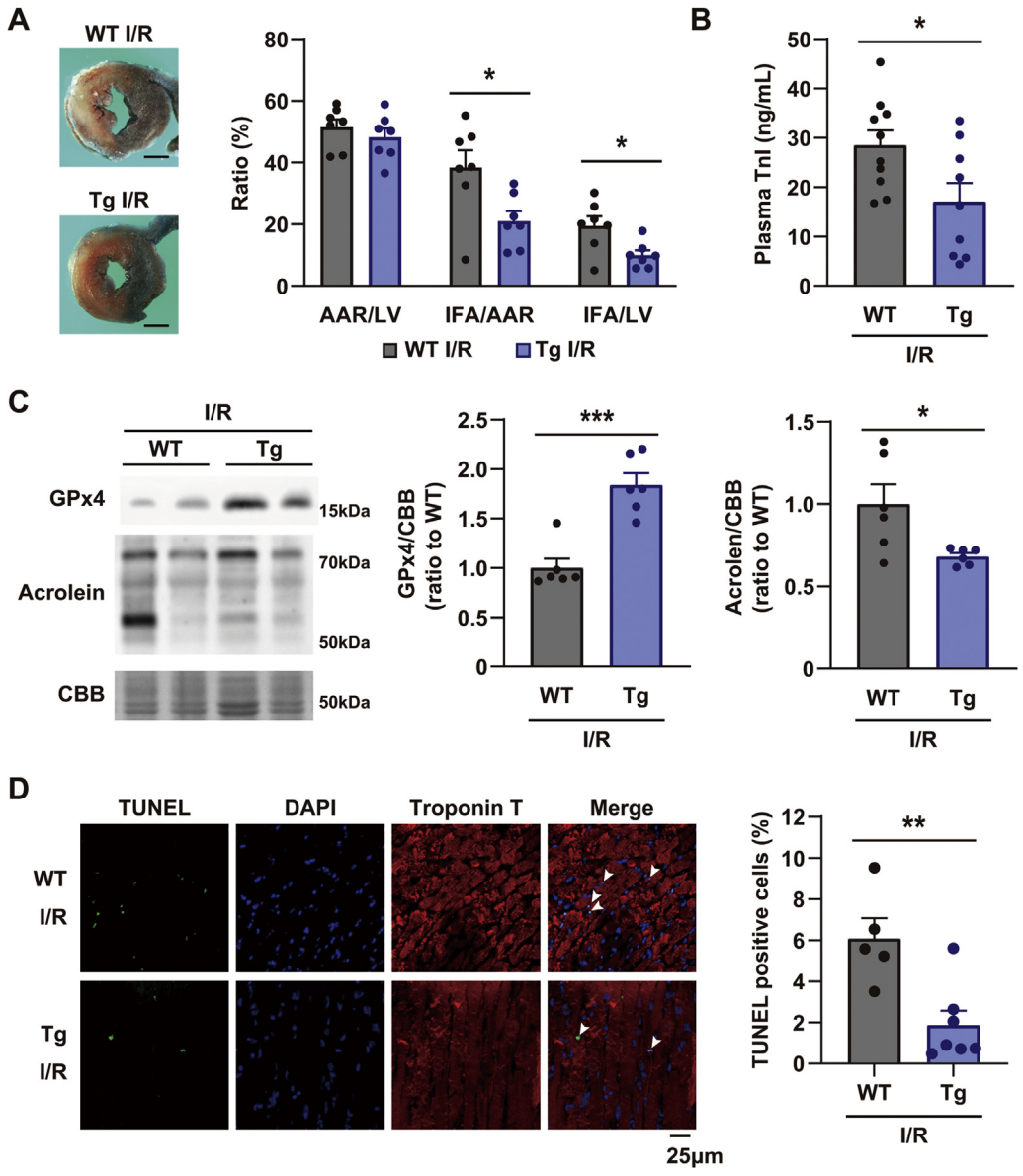

(A) (left) Representative images of I/R myocardium in WT and GPx4 Tg mice, double-stained by TTC and Evans Blue. Scale bar = 1 mm. **(right)** The percentages of area at risk (AAR) per left ventricle (LV), infarct area (IFA) per AAR, and IFA per LV in WT and GPx4 Tg mice 24 hours after reperfusion (n = 7). **(B)** Plasma troponin I (TnI) levels (n = 9-10) 24 hours after reperfusion. **(C) (left)** Western blot of GPx4 and acrolein levels in the heart tissue lysates of I/R-injured myocardium from WT and GPx4 Tg mice; **(right)** quantification of Western blot results (n = 6). Each band intensity was standardized to Coomassie Brilliant Blue (CBB) staining (50 kDa). **(D) (left)** Representative images of TUNEL staining **(green)** and co-staining with DAPI **(blue)** and troponin T **(red)**, and **(right)** the number of TUNEL and DAPI double-positive nuclei in troponin T-positive myocardium 24 hours after reperfusion (n = 5-7). Scale bar = 25 μm; **arrowheads** indicate TUNEL-positive nuclei. Data are shown as mean ± SEM. Statistical significance was determined by means of Student's *t*-test. *$P < 0.05$; **$P < 0.01$; ***$P < 0.001$. Tg = transgenic; TTC = triphenyltetrazolium chloride; WT = wild-type; other abbreviations as in Figure 1.

transmembrane potential and causing cytochrome c release and MPT-driven necrosis.[34,35] Because both ferroptosis and MPT-driven necrosis are triggered by oxidative stress, the role of ferroptosis in myocardial I/R injury was examined in comparison with MPT-driven necrosis. Treatment with CsA or GPx4 overexpression equally reduced the infarct size compared with that in I/R-injured mice without intervention

FIGURE 3 **Heterodeletion of GPx4 Aggravated Myocardial I/R Injury**

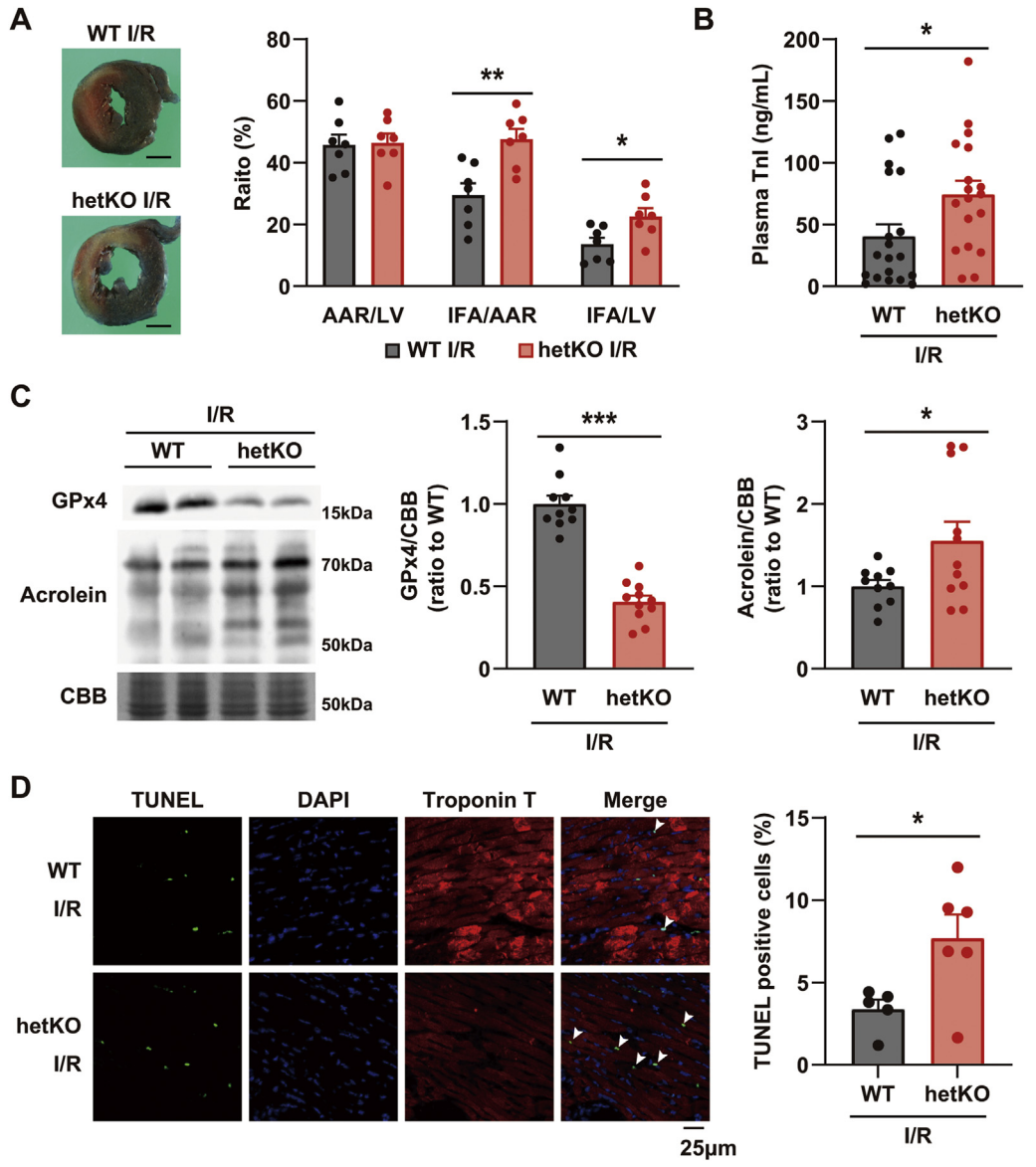

(A) (left) Representative images of I/R myocardium in WT and hetKO mice, double-stained by TTC and Evans Blue. Scale bar = 1 mm (left panel). **(right)** The percentages of area at risk (AAR) per left ventricle (LV), infarct area (IFA) per AAR, and IFA per LV in WT and hetKO mice 24 hours after reperfusion (n = 7). **(B)** Plasma troponin I (TnI) levels 24 hours after reperfusion (n = 18-19). **(C) (left)** Western blot of GPx4 and acrolein levels in the heart tissue lysates of I/R-injured myocardium from WT and hetKO mice 15 hours after reperfusion; **(right)** quantification of Western blot results (n = 10-11). Each band intensity was standardized to Coomassie Brilliant Blue (CBB) staining (50 kDa). **(D) (left)** Representative images of TUNEL staining **(green)** and co-staining with DAPI **(blue)** and troponin T **(red)**, and (right) the number of TUNEL and DAPI double-positive nuclei in troponin T–positive myocardium 24 hours after reperfusion (n = 5-6). Scale bar = 25 μm; **arrowheads** indicate TUNEL-positive nuclei. Data are shown as mean ± SEM. Statistical significance was determined by means of Student's *t*-test. *$P < 0.05$; **$P < 0.01$; ***$P < 0.001$. hetKO = GPx4 hetero-knockout; other abbreviations as in Figures 1 and 2.

(Figures 4A and 4B). Of note, CsA additionally reduced the infarct size in GPx4 Tg mice, and the sum of the percentage reductions by GPx4 Tg and CsA treatment was equal to that of concomitant inhibition of ferroptosis and MPT-driven necrosis (Figure 4C), suggesting that ferroptosis is a distinct cell death mode from MPT-driven necrosis in myocardial I/R injury, and that there is no overlap between

FIGURE 4 Ferroptosis Was a Cell Death Mode Distinct From MPT-Driven Necrosis in Myocardial I/R Injury

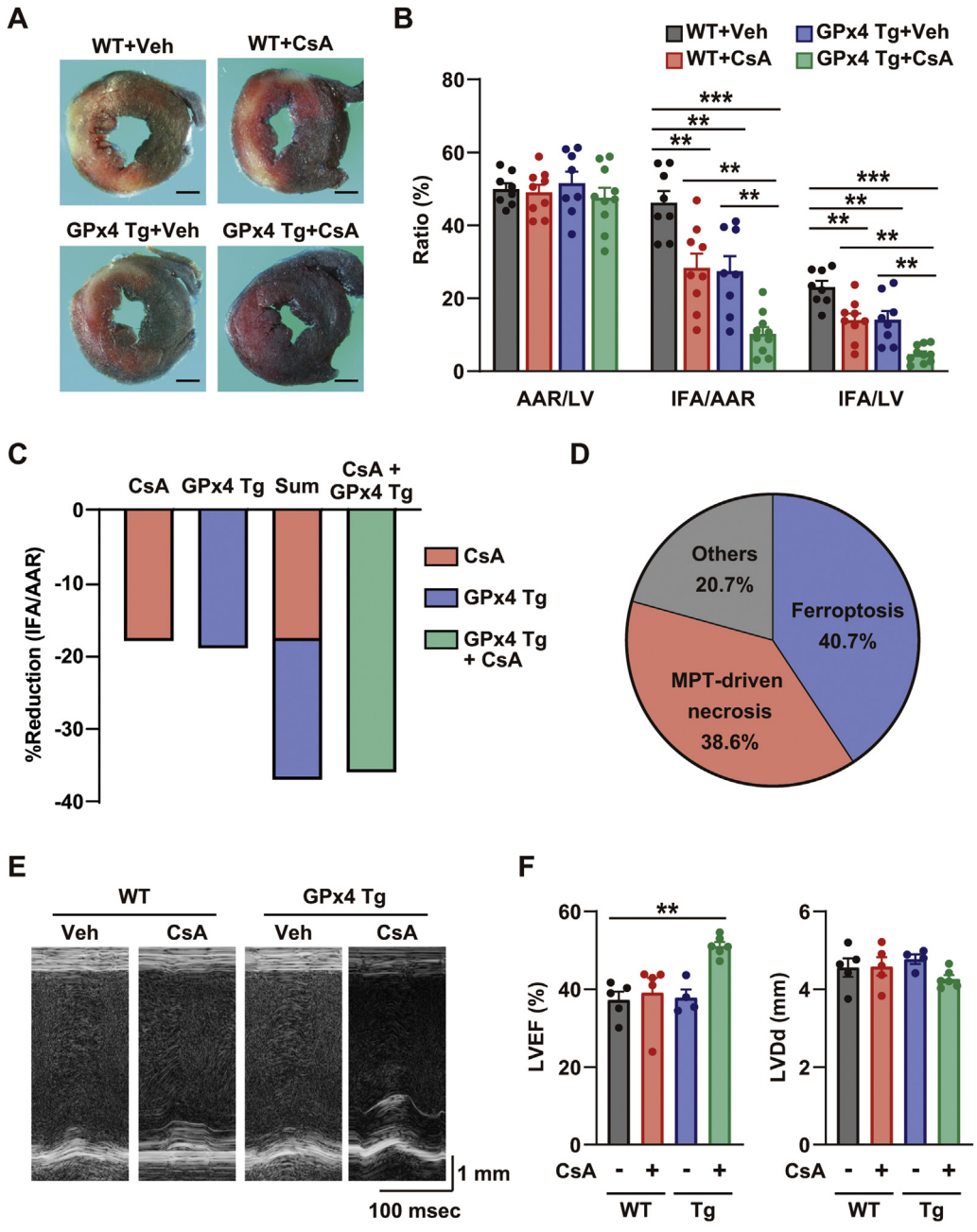

(A) Representative images of double-staining by TTC and Evans Blue. **(B)** The percentages of area at risk (AAR) per left ventricle (LV), infarct area (IFA) per AAR, and IFA per LV in either WT with vehicle, WT with CsA, GPx4 Tg with vehicle, and GPx4 Tg with CsA mice 24 hours after reperfusion (n = 8-10). **(C)** Reduction of infarct size in CsA, GPx4 Tg, and GPx4 Tg with CsA mice. **(D)** Ratio of ferroptosis, MPT-driven necrosis, and other cell death in myocardial I/R injury. **(E)** Representative images of M-mode echocardiography on day 14 after I/R. **(F)** Left ventricular ejection fraction (LVEF) and left ventricular diameter in diastole (LVDd) (n = 4-6). Data are shown as mean ± SEM. Statistical significance was determined by means of **(B)** 1-way analysis of variance with post hoc Tukey's honest significance difference test and **(F)** Dunnett's test (vs WT with vehicle). $^{**}P < 0.01$; $^{***}P < 0.001$. CsA = cyclosporine A; MPT = mitochondrial permeability transition; other abbreviations as in Figures 1 and 2.

ferroptosis and MPT-driven necrosis. The relative in vivo contributions of ferroptosis and MPT-driven necrosis in myocardial I/R injury are summarized in **Figure 4D** based on the above findings. Moreover, the combination of GPx4 overexpression and CsA treatment significantly improved the LVEF on day 14 after I/R, whereas GPx4 overexpression or CsA treatment did not (**Figures 4D and 4E**). In contrast, heterodeletion of GPx4 aggravated the impairment of LVEF and cardiac dilation on day 14 after I/R (Supplemental Figures 3A and 3B). These results confirmed the major role of ferroptosis in infarct size and cardiac function during the early and late phases after I/R, respectively.

FERROPTOSIS WAS INDUCED BY H/R IN CULTURED CARDIOMYOCYTES. To further investigate the molecular basis of ferroptosis in myocardial I/R injury, cultured cardiomyocytes stimulated by H/R were examined. Consistent with the in vivo myocardial I/R injury findings, both GPx4 transcription and protein levels were significantly decreased in response to either Hx or H/R (**Figures 5A and 5B**). H/R increased the levels of LPs probed with C11-BODIPY and induced cell death in cultured cardiomyocytes (**Figures 5C to 5E**). Treatment with Fer-1 (a competent inhibitor of ferroptosis) or DXZ (an iron chelator) significantly suppressed the levels of LPs and prevented cell death induced by H/R (**Figures 5C to 5E**). This was also confirmed in adult cardiomyocytes (**Figure 5F**). Collectively, ferroptosis was a major mode of RCDs induced by H/R in cultured cardiomyocytes.

FERROPTOSIS FOLLOWING H/R WAS PREVENTED BY CYTOSOLIC, NOT MITOCHONDRIAL, GPx4. To investigate the role of GPx4 and identify the pivotal organelle in ferroptosis after H/R, we used Ad-cytoGPx4 and Ad-mitoGPx4 with a mitochondrial targeting signal as described previously.[18] Indeed, these GPx4 adenoviruses increased the GPx4 level in a multiplicity of infection-dependent manner (**Figures 6A and 6B,** Supplemental Figures 4A and 4B). The overexpression of cytosolic *Gpx4* suppressed the levels of LPs, and effectively prevented ferroptosis after H/R, whereas mitochondrial *Gpx4* expression had no significant protection against ferroptosis induced by H/R (**Figures 6C to 6E**). These results suggest that ferroptosis in response to H/R is triggered in organelles, excluding the mitochondria.

IRON OVERLOAD IN ER TRIGGERED FERROPTOSIS IN H/R. Total cellular iron was not changed at 4 hours after Hx according to the 2 methods, ferrozine method with whole cell lysates (**Figure 7A**) and fluorescent imaging with the use of FerroOrange (Supplemental Figure 5A). We then examined the Fe^{2+} level in the ER of cultured cardiomyocytes with the use of FFR, a specific fluorescence probe for Fe^{2+} in the ER, as Cui et al[36] recently demonstrated that Hx elevates the Fe^{2+} level in the ER with the use of this probe[37,38] and Kagan et al[39] reported that the ER is associated with ferroptosis in GPx4-deficient Pfa1 cells. This examination revealed that the fluorescence detected by FFR was merged with that of ERseeing, a specific indicator for the ER, and Fe^{2+} levels were markedly enhanced in the ER under Hx, compared with normoxia (Nx) (**Figure 7B**). Furthermore, this enhancement was significantly suppressed by DXZ treatment (**Figure 7B**). Consistently, iron was significantly increased in the ER-enriched fraction of I/R-injured myocardium compared with that of the sham-operated myocardium (**Figure 7C**). Furthermore, Fe^{2+} overload in ER induced by Hx was also observed in adult cardiomyocytes (**Figure 7D**). Pretreatment using FFR as a chelator for iron in ER, but not MFG (a specific chelator for Fe^{2+} in mitochondria), significantly suppressed the LP levels and prevented H/R-induced ferroptosis (**Figures 7E and 7F,** Supplemental Figure 5B).

HO-1 INDUCED IRON OVERLOAD IN THE ER AND TRIGGERED FERROPTOSIS FOLLOWING H/R. HO-1, up-regulated in response to various stresses and localized at the ER, causes heme degradation and produces Fe^{2+} accompanied by biliverdin and carbon monoxide.[40] Indeed, the HO-1 levels were increased in the I/R-injured myocardium at 6 hours and 24 hours after reperfusion (**Figure 8A**) and in cultured cardiomyocytes after Hx and H/R (**Figure 8B**). Therefore, we finally examined the effect of HO-1 silencing on iron overload, LPs, and ferroptosis induced by H/R. Interestingly, silencing HO-1 abolished the iron overload in the ER (**Figures 8C and 8D**), suppressed an increase in the levels of LPs (**Figure 8E**), and prevented ferroptosis induced by H/R (**Figure 8F**). Collectively, HO-1 up-regulation in response to Hx and H/R degraded heme and thereby induced Fe^{2+} accumulation in the ER, triggering ferroptosis after H/R.

DISCUSSION

I/R injury remains a critical concern, and therapeutics for reperfusion injury have yet to be established. Analyzing genetically engineered mice and using adenoviruses harboring *Gpx4* and specific pharmacologic interventions, we obtained 3 major findings in this study: 1) GPx4 is a key regulator of ferroptosis in myocardial I/R injury; 2) ferroptosis operates

FIGURE 5 Ferroptosis Was Induced by H/R in Cultured Cardiomyocytes

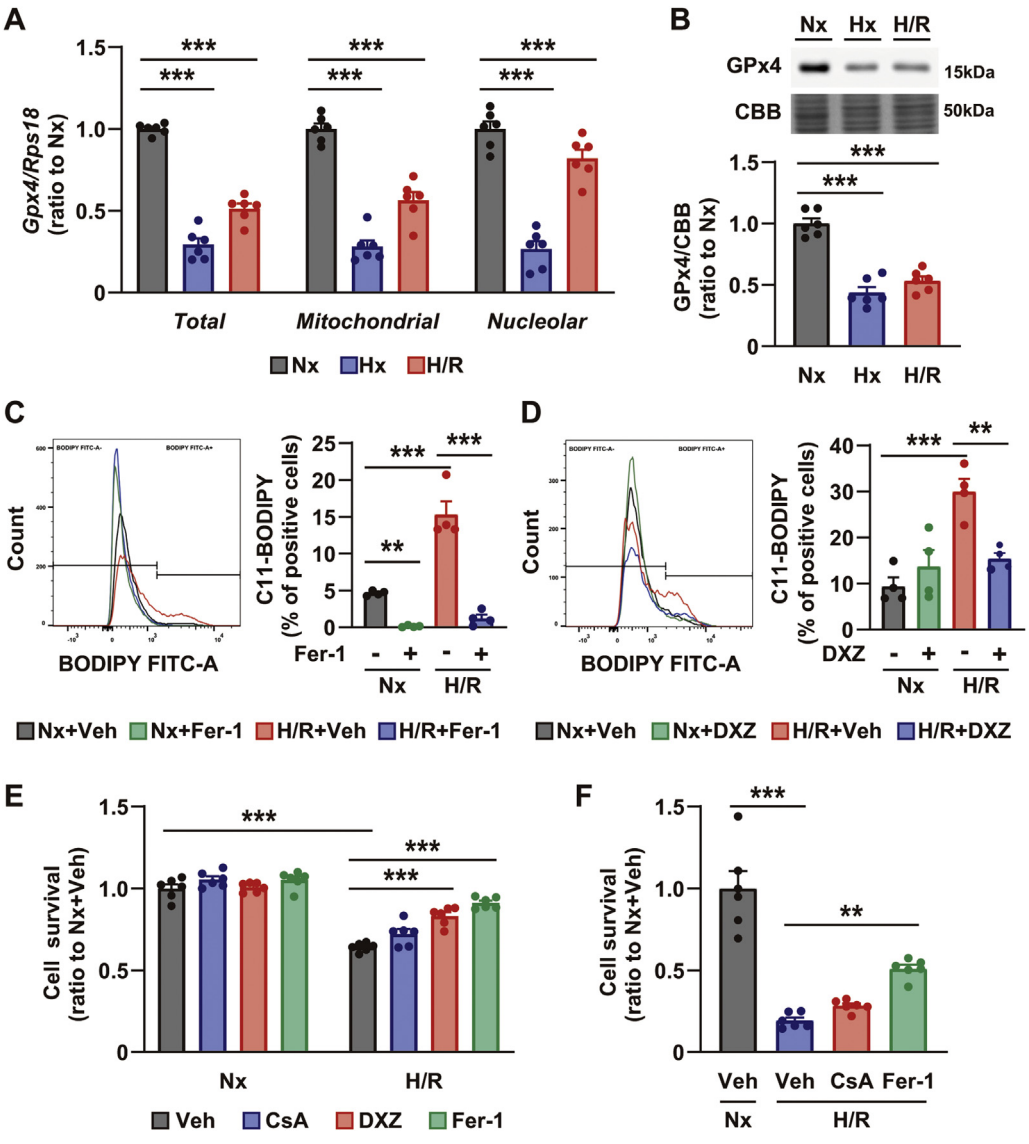

(A) Gene expression of total, mitochondrial, and nucleolar *Gpx4* following either hypoxia (Hx) or H/R (24 h hypoxia and 6 h reoxygenation) in cultured cardiomyocytes (n = 6). **(B) (top)** Western blot of GPx4 levels in the cultured cardiomyocytes after 24 hours of Hx or H/R (24 h hypoxia and 6 h reoxygenation). **(bottom)** Quantification of Western blot results (n = 6). Each band intensity was standardized to Coomassie Brilliant Blue (CBB) staining (50 kDa). **(C) (left)** Histogram of flow-cytometric analysis for lipid peroxides, probed with the use of C11-BODIPY in cultured cardiomyocytes after H/R, treated with either vehicle or Fer-1 (50 μmol/L); **(right)** ratio of C11-BODIPY-positive cells in flow-cytometric (for overall consistency) analysis (n = 4). **(D) (left)** Histogram of flow-cytometric analysis for lipid peroxides, probed with the use of C11-BODIPY in cultured cardiomyocytes after H/R, treated with either vehicle or DXZ (1 mmol/L); **(right)** ratio of C11-BODIPY-positive cells in flow-cytometric analysis (n = 4). **(E)** Cell survival after Nx and H/R in cultured cardiomyocytes treated with either vehicle, CsA (2 μmol/L), DXZ (1 mmol/L), or Fer-1 (50 μmol/L) (n = 6). **(F)** Cell survival after Nx and H/R in adult cardiomyocytes treated with either CsA (2 μmol/L) or Fer-1 (50 μmol/L) (n = 6). Data are shown as mean ± SEM. Statistical significance was determined by means of **(C to F)** 1-way analysis of variance with post hoc Tukey's honest significance difference test and **(A and B)** Dunnett's test (vs Nx). $^{**}P < 0.01$, $^{***}P < 0.001$. DXZ = dexrazoxane; Fer-1 = ferrostatin=1; H/R = hypoxia-reoxygenation; Hx = hypoxia; Nx = normoxia; other abbreviations as in Figures 1 and 4.

FIGURE 6 Ferroptosis After H/R Was Prevented by Cytosolic GPx4 but Not Mitochondrial GPx4

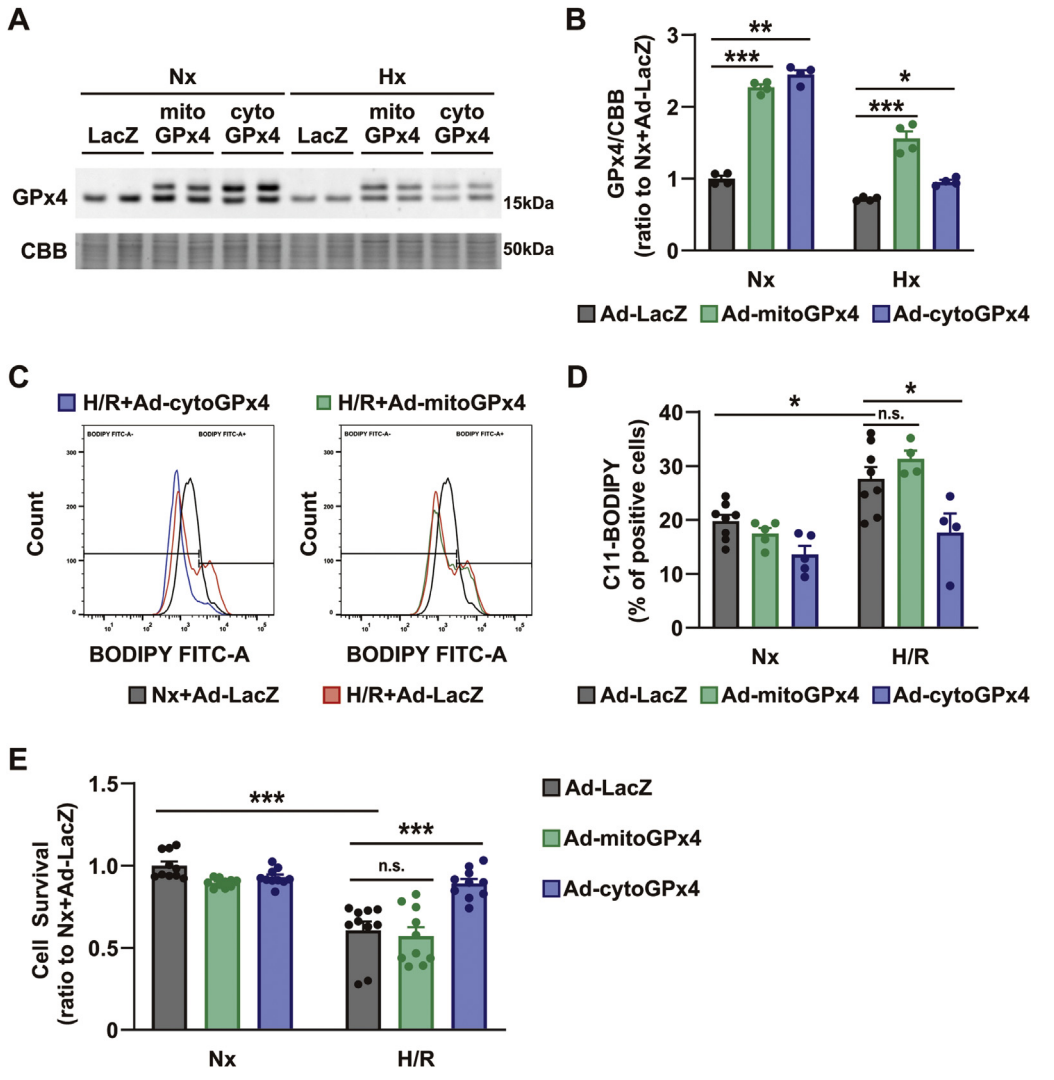

(A) Western blot of GPx4 level in the cultured cardiomyocytes transfected with Ad-cytoGPx4 (5 MOI) and Ad-mitoGPx4 (5 MOI) after 24 hours of hypoxia. **(B)** Quantification of Western blot results shown in **A** (n = 4). Each band intensity was standardized to Coomassie Brilliant Blue (CBB) staining (50 kDa). **(C)** Histograms of flow-cytometric analysis for lipid peroxides, probed →with the use of C11-BODIPY in cultured cardiomyocytes following H/R, infected with **(left)** Ad-cytoGPx4 and **(right)** Ad-mitoGPx4. **(D)** Ratio of C11-BODIPY–positive cells in flow-cytometric analysis as shown in **C** (n = 4-8). **(E)** Cell survival after H/R in cultured cardiomyocytes infected with Ad-cytoGPx4 and Ad-mitoGPx4 (n = 10). Data are shown as mean ± SEM. Statistical significance was determined by means of 1-way analysis of variance with post hoc Tukey's honest significance difference test. *$P < 0.05$; **$P < 0.01$; ***$P < 0.001$. Ad-cytoGPx4 = adenovirus harboring cytosolic *Gpx4*; Ad-mitoGPx4, adenovirus harboring mitochondrial *Gpx4*; Ad-LacZ = adenovirus encoding reporter gene *LacZ*; other abbreviations as in Figures 1, 4, and 5.

independently from MPT-driven necrosis, and therapeutics targeting both ferroptosis and MPT-driven necrosis could achieve additional cardioprotection in I/R injury; and 3) iron overload in the ER through heme degradation by HO-1 causes H/R-induced ferroptosis in cardiomyocytes. Our findings suggest that hypoxic response causes GPx4 reduction and HO-1 up-regulation, thereby triggering ferroptosis in I/R-injured myocardium through iron overload in the ER.

Ferroptosis is defined as an RCD that is under constitutive control by GPx4.[10] GPx4 determines the susceptibility to ferroptosis, with its reduction resulting in ferroptosis even if iron homeostasis is physiologically maintained.[14] In the present study,

FIGURE 7 Hypoxia Induced Iron Overload in ER

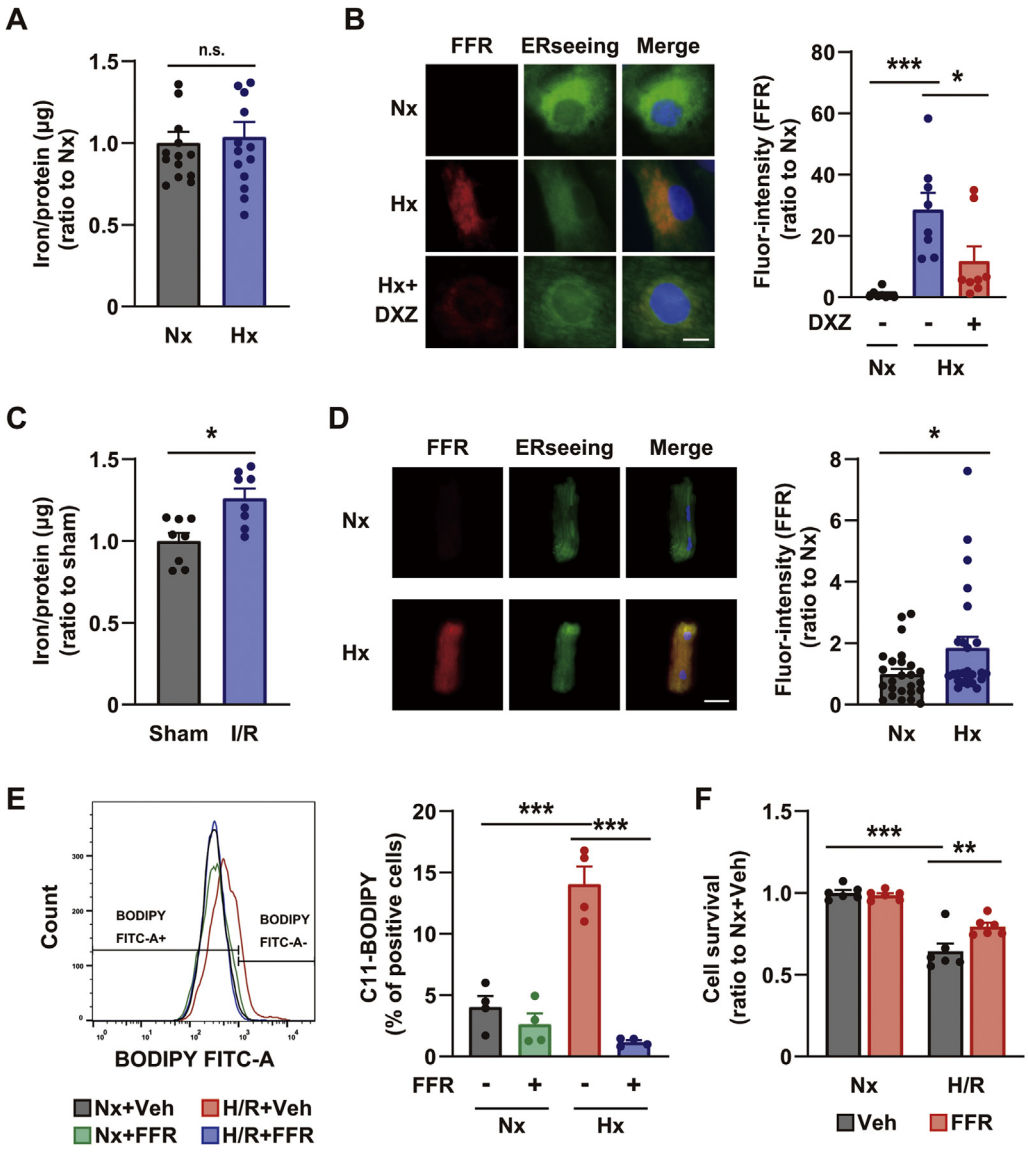

(A) Total cellular iron in cultured cardiomyocytes after 4 hours of Hx according to the ferrozine method (n = 13). **(B) (left)** Representative fluorescence imaging of iron in the ER with the use of FFR **(red)** in cultured cardiomyocytes after 4 hours of Hx. The ER and nucleus in cultured cardiomyocytes were counterstained with ERseeing **(green)** and DAPI **(blue)**, respectively. Scale bar = 10 μm. **(right)** Quantification of the relative intensity of FFR in cultured cardiomyocytes (n = 8). **(C)** Iron content in ER fractions extracted from I/R-injured myocardium (n = 8). **(D) (left)** Representative fluorescence imaging of iron in the ER with the use of FFR **(red)** in adult mouse cardiomyocytes, after 4 hours of Hx. The ER and nucleus in adult cardiomyocytes were counterstained with ERseeing **(green)** and DAPI **(blue)**, respectively. Scale bars = 25 μm. **(right)** Quantification of the relative intensity of FFR in cultured cardiomyocytes (n = 25). **(E) (left)** Histogram of flow-cytometric analysis for lipid peroxides, probed with the use of C11-BODIPY in cultured cardiomyocytes treated with FFR after H/R; **(right)** ratio of C11-BODIPY–positive cells in flow-cytometric analysis (n = 4). **(F)** Cell survival after H/R in cultured cardiomyocytes treated with FFR (10 μmol/L) (n = 6). Data are shown as mean ± SEM. Statistical significance was determined by means of **(A, C, D)** Student's *t*-test and **(B, E, F)** 1-way analysis of variance with post hoc Tukey's honest significance difference test **(B, E, F)**. *$P < 0.05$; **$P < 0.01$; ***$P < 0.001$. ER = endoplasmic reticulum; FFR = FerroFarRed; other abbreviations as in Figures 1, 4, and 5.

FIGURE 8 **HO-1 Up-regulation Induced Iron Overload in ER and Triggered Ferroptosis in H/R**

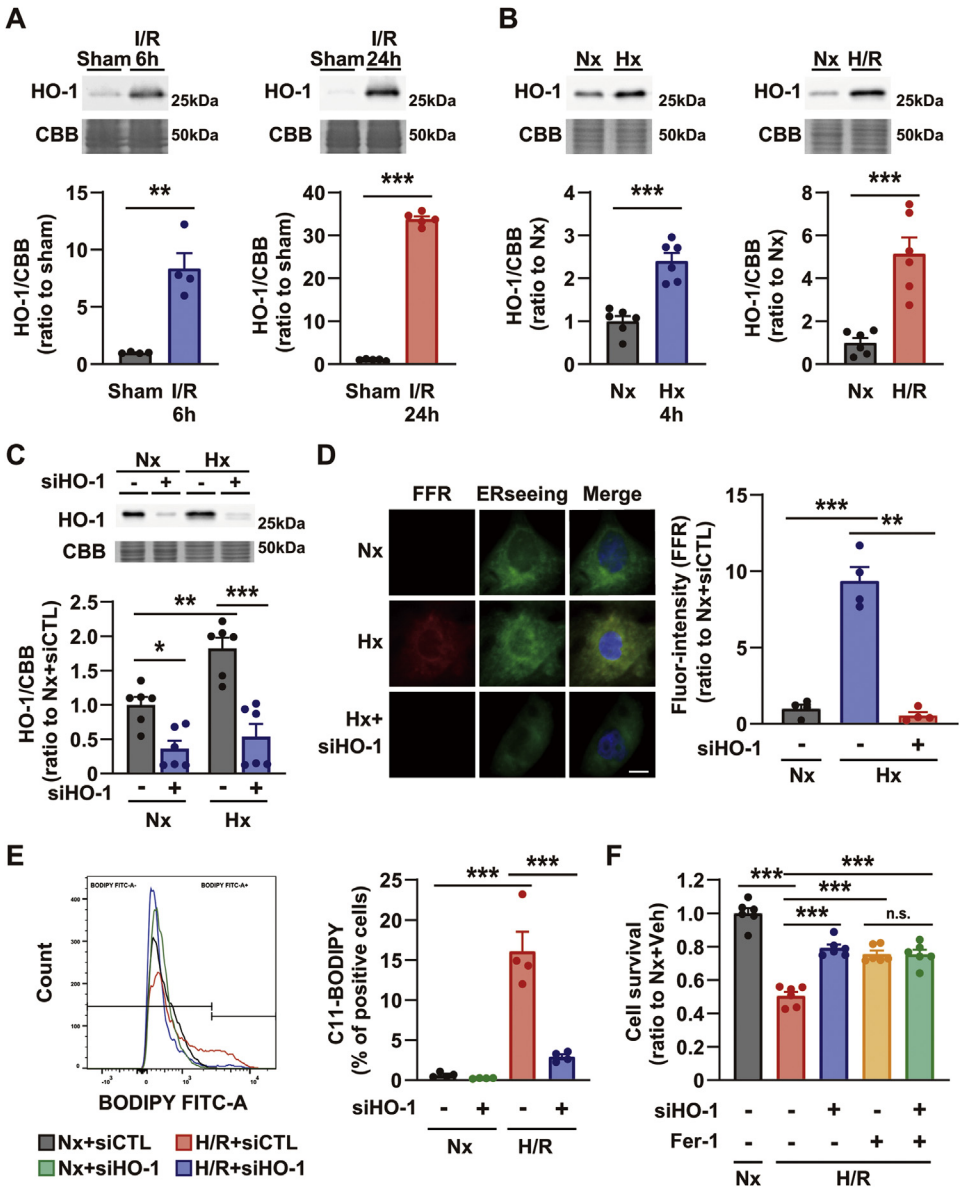

(A) (top) Western blot of HO-1 levels in the area at risk of respective hearts **(left)** 6 hours (n = 4) and **(right)** 24 hours after reperfusion (n = 5); **(bottom)** quantification of Western blot results. Each band intensity was standardized to CBB staining (50 kDa). **(B) (top)** Western blot of HO-1 in the cultured cardiomyocytes after **(left)** Hx (n = 6) and **(right)** H/R (n = 6). **(bottom)** Quantification of Western blot results. Each band intensity was standardized to CBB staining (50 kDa). **(C) (top)** Western blot of HO-1 in the cultured cardiomyocytes after 4 hours of Hx, transfected with siHO-1; **(bottom)** quantification of Western blot results (n = 6). Each band intensity was standardized to CBB staining (50 kDa). **(D) (left)** Representative fluorescence imaging of iron in the ER with the use of FFR **(red)** in cultured cardiomyocytes transfected with siHO-1 after 4 hours of Hx. ER in cultured cardiomyocytes were counterstained with ERseeing **(green)** and DAPI **(blue)**. Scale bar = 10 μm. **(right)** Quantification of the relative intensity of FFR in cultured cardiomyocytes (n = 4). **(E) (left)** Histogram of flow-cytometric analysis for lipid peroxides, probed with the use of C11-BODIPY in cultured cardiomyocytes transfected with siHO-1 after H/R; **(right)** ratio of C11-BODIPY-positive cells in flow-cytometric analysis (n = 4). **(F)** Cell survival after H/R in cultured cardiomyocytes transfected with siHO-1 and/or treated with Fer-1 (n = 6). Data are shown as mean ± SEM. Statistical significance was determined by means of **(A and B)** Student's *t*-test and **(C to F)** 1-way analysis of variance with post hoc Tukey's honest significance difference test. *$P < 0.05$; **$P < 0.01$; ***$P < 0.001$. CCB = Coomassie Brilliant Blue; HO-1 = heme oxygenase 1; siHO-1 = small interfering RNA targeting *Hmox-1*; other abbreviations as in Figures 1, 4, 5, and 7.

JACC: BASIC TO TRANSLATIONAL SCIENCE VOL. 7, NO. 8, 2022
AUGUST 2022:800–819

we showed that GPx4 levels were reduced in both I/R-injured myocardium and cultured cardiomyocytes under H/R. We also demonstrated that the overexpression of GPx4 reduced the infarct size in myocardial I/R injury, whereas the hetero-deletion of GPx4 aggravated it. In addition, we showed that the overexpression of cytosolic GPx4 suppressed cell death induced by H/R. Taken together, these results suggest that ferroptosis is a major mode of RCD, and GPx4 is implicated as a critical regulator of ferroptosis in myocardial I/R injury.

Ferroptosis is an RCD triggered by LPs, which are one of the final products initiated by oxidative stress. Given that MPT-driven necrosis is also triggered by oxidative stress, we initially hypothesized that ferroptosis and MPT-driven necrosis partially share a common signaling pathway in myocardial I/R injury. However, in the present study, GPx4 overexpression showed an additional benefit against myocardial I/R injury in conjunction with CsA treatment. Furthermore, cell death induced by H/R could not be prevented by CsA treatment in cultured cardiomyocytes, whereas this cell death was fully prevented by both cytosolic Gpx4 overexpression and Fer-1 treatment (**Figures 5 and 6**), implicating ferroptosis as the major mode of cell death after H/R. To investigate the potentially overlapping mechanism of ferroptosis and MPT-driven necrosis, we examined the membrane potential in GPx4-deficient cardiomyocytes with the use of siRNA. We found that the membrane potential was also reduced in GPx4-deficient ferroptosis, as observed in cardiomyocytes treated with the protonophore m-chlorophenylhydrazone, an MPT-driven necrosis inducer (Supplemental Figures 6A and 6B). However, CsA treatment did not prevent ferroptosis induced by silencing GPx4 (Supplemental Figure 6C). Collectively, ferroptosis is distinct from MPT-driven necrosis, and the loss of membrane potential is not a cause of ferroptosis and is simply observed in ferroptosis as a common feature of cell death. This is consistent with the findings that Fer-1, but not CsA, prevents H/R-induced ferroptosis in neonatal and adult cardiomyocytes (**Figures 5E and 5F**). Our findings suggest that ferroptosis is the predominant mode of cell death in myocardial I/R injury as well as MPT-driven necrosis, indicating that ferroptosis is a promising therapeutic target in conjunction with CsA treatment.

The organelle responsible for ferroptosis initiation remains unclear. We first examined the role of the mitochondria with the use of Ad-mitoGPx4 because we initially hypothesized that ferroptosis uses the common machinery of MPT-driven necrosis. However, the present study demonstrated that H/R-induced ferroptosis was not inhibited by mitochondrial Gpx4 and mitochondria-targeting iron chelation (**Figure 6E,** Supplemental Figure 5B), whereas it could be fully prevented by cytosolic Gpx4 overexpression, suggesting that ferroptosis is triggered in organelles, excluding the mitochondria. To identify the pivotal organelle responsible for H/R-induced ferroptosis, we examined the iron levels in the ER, and found an increase in Fe^{2+} levels in the ER with the use of FFR, which specifically targets the ER. Consistent with this finding, the iron overload in ER was also confirmed in I/R-injured myocardium and adult cardiomyocytes under Hx. Furthermore, FFR treatment for chelating Fe^{2+} in the ER prevented H/R-induced ferroptosis. These results suggest that Hx and H/R increase iron levels in the ER and implicate the ER as a pivotal organelle in H/R-induced ferroptosis.

HO-1 is an enzyme that catalyzes the degradation of heme to produce Fe^{2+} as well as biliverdin and carbon monoxide. It is localized mainly at the ER and regulated by various stresses, including Hx. In the present study, we demonstrated that silencing HO-1 abolished both the iron overload and increase in LP levels, while preventing ferroptosis induced by H/R. This suggests that heme degradation through HO-1 up-regulation causes iron overload in the ER and induces ferroptosis. To identify the molecule responsible for iron overload in ER, we also investigated the other potential mechanism underlying iron overload in Hx. Indeed, the expression of transferrin receptor 1 (*Tfrc*), an importer of cellular iron, was upregulated in cultured cardiomyocytes after 4 hours of Hx (Supplemental Figure 7A). However, silencing *Tfrc* is not effective for abolishing iron overload in ER under Hx (Supplemental Figures 7B and 7C). In addition, the expression of ferroportin (*Slc40a1*), an exporter of cellular iron, was downregulated in cultured cardiomyocytes after 4 hours of Hx (Supplemental Figure 8A). Moreover, silencing *Slc40a1* reduced its transcription 4 hours after siRNA transfection as well as after 4 hours of Hx, but did not reproduce the iron overload in ER (Supplemental Figures 8B and 8C). Thus, we could not find evidence that transferrin and ferroportin are involved in iron overload in ER in our preparations. Nevertheless, they might be directly or indirectly responsible, in part, for iron overload under Hx in other preparations.

HO-1 has an established role in cardioprotection during I/R injury.[41] Indeed, a detailed analysis of HO-1 in an I/R injury model by Yet et al[42] showed that cardiac-specific overexpression of HO-1 reduces infarct size, suggesting that the overall outcome of

HO-1 is protective against I/R injury. In this context, the newly uncovered role of HO-1 in ferroptosis in I/R injury was intriguing for therapeutic strategy against I/R injury. Considering that several studies have confirmed the cardioprotective role of HO-1 against I/R injury by reducing oxidative stress through biliverdin and carbon monoxide,[43,44] our results do not overturn its cardioprotective role in I/R injury. However, the present findings do uncover the detrimental aspect of HO-1 in I/R injury, masked by favorable consequence through HO-1 up-regulation. Understanding the negative role of HO-1 in ferroptosis would be beneficial for the development of therapeutics by gain of function in HO-1 in I/R injury,[45] because HO-1 overexpression can potentially promote ferroptosis, thereby minimizing its cardioprotection in I/R injury. Therefore, concomitant therapy targeting ferroptosis can maximize the cardioprotection induced by gain of function in HO-1.

STUDY LIMITATIONS. We acknowledge 2 major limitations of this study. First, we used genetically engineered mice in which *Gpx4* was globally deleted or inserted in the mouse genome. Therefore, the ferroptosis in some cells, excluding cardiomyocytes, or tissues in the I/R model may be partly responsible for the cardiac phenotypes in these mice. Second, we did not find a significant cardioprotective effect against H/R-induced cell death by CsA in cardiomyocytes in vitro (**Figures 5E and 5F**), although ferroptosis and MPT-driven necrosis are equally responsible for myocardial I/R injury in mice in vivo (**Figure 4D**). To examine ferroptosis in comparison with MPT-driven necrosis in vitro, hydrogen peroxide (H_2O_2) was also used to mimic the I/R injury in cultured cardiomyocytes, as previously described.[8,9] However, ferroptosis was the dominant form of cell death on H_2O_2 treatment, and the cardioprotective effect of CsA for cell survival was slight and nonsignificant against H_2O_2-induced cell death (Supplemental Figure 9). Thus, we could not accurately reproduce MPT-driven necrosis in vitro and evaluate ferroptosis compared with MPT-driven necrosis in cardiomyocytes.

CONCLUSIONS

Hx and H/R result in GPx4 down-regulation and HO-1 up-regulation, both of which work cooperatively to trigger ferroptosis in I/R injury through iron overload in the ER. Furthermore, ferroptosis in I/R injury is distinct from MPT-driven necrosis at both phenotypic and molecular levels, and therapeutics targeting ferroptosis in conjunction with CsA can be a promising strategy for myocardial I/R injury.

ACKNOWLEDGMENTS The authors thank Midori Sato and Akiko Hanada for their excellent technical assistance.

FUNDING SUPPORT AND AUTHOR DISCLOSURES

This work was supported by JSPS KAKENHI (grants JP16H07049, JP18K15892, and JP21K16090 to Dr Ikeda; JP20K08426 to Dr Ide; and JP18K19405 and JP20H00493 to Dr Yamada), Uehara Memorial Foundation (to Dr Ikeda), the Japan Foundation for Applied Enzymology (VBIC: Vascular Biology of Innovation; to Dr Ikeda), MSD Life Science Foundation, the Public Interest Incorporated Foundation (to Dr Ikeda); Novartis Pharma Grants for Basic Research 2020 (to Dr Ikeda), Kowa Life Science Foundation (to Dr Ikeda); Center for Clinical and Translational Research of Kyushu University Hospital (to Dr Ide), and AMED-CREST (grant JP21gm0910013 to Drs Yamada and Imai). Dr Tsutsui has received remunerations from Kowa, Teijin Pharma, Nippon Boehringer Ingelheim, Mitsubishi Tanabe Pharma, Pfizer Japan, Ono Pharmaceutical, Daiichi Sankyo, Novartis Pharma, Bayer Yakuhin, Otsuka Pharmaceutical, and AstraZeneca; manuscript fee from Nippon Rinsho; research funding from Mitsubishi Tanabe Pharma, Nippon Boehringer Ingelheim, IQVIA Services Japan, MEDINET, Medical Innovation Kyushu, Kowa, Daiichi Sankyo, Johnson & Johnson, and NEC Corp; and scholarship funds or donations from Abbott Medical Japan, Otsuka Pharmaceutical, Boston Scientific Japan, Ono Pharmaceutical, Bayer Yakuhin, Nippon Boehringer Ingelheim, St Mary's Hospital, Teijin Pharma, Daiichi Sankyo, and Mitsubishi Tanabe Pharma. All other authors have reported that they have no relationships relevant to the contents of this paper to disclose.

ADDRESS FOR CORRESPONDENCE: Dr Masataka Ikeda or Dr Tomomi Ide, Department of Cardiovascular Medicine, Faculty of Medical Sciences, Kyushu University, 3-1-1 Maidashi, Higashi-ku, Fukuoka 812-8582, Japan. E-mail: ikeda-m@cardiol.med.kyushu-u.ac.jp OR tomomi_i@cardiol.med.kyushu-u.ac.jp.

PERSPECTIVES

COMPETENCY IN MEDICAL KNOWLEDGE: Ferroptosis is a mode of cell death distinct from MPT-driven necrosis in both in vivo phenotype and in vitro mechanism in myocardial I/R injury. Ferroptosis is triggered by iron overload in the ER via heme degradation by HO-1 up-regulation.

TRANSLATIONAL OUTLOOK: Inhibition of ferroptosis offers marked cardioprotection even under CsA treatment in I/R injury, suggesting that therapeutics targeting ferroptosis in conjunction with CsA can be a promising strategy for I/R injury.

REFERENCES

1. Writing Group Members, Mozaffarian D, Benjamin EJ, Go AS, et al. Heart disease and stroke statistics—2016 update: a report from the American Heart Association. *Circulation*. 2016;133:e38–e360.

2. Fibrinolytic Therapy Trialists' (FTT) Collaborative Group. Indications for fibrinolytic therapy in suspected acute myocardial infarction: collaborative overview of early mortality and major morbidity results from all randomised trials of more than 1000 patients. *Lancet*. 1994;343:311–322.

3. Keeley EC, Boura JA, Grines CL. Primary angioplasty versus intravenous thrombolytic therapy for acute myocardial infarction: a quantitative review of 23 randomised trials. *Lancet*. 2003;361:13–20.

4. Velagaleti RS, Pencina MJ, Murabito JM, et al. Long-term trends in the incidence of heart failure after myocardial infarction. *Circulation*. 2008;118:2057–2062.

5. Braunwald E, Kloner RA. Myocardial reperfusion: a double-edged sword? *J Clin Invest*. 1985;76:1713–1719.

6. Di Lisa F, Menabo R, Canton M, Barile M, Bernardi P. Opening of the mitochondrial permeability transition pore causes depletion of mitochondrial and cytosolic NAD+ and is a causative event in the death of myocytes in postischemic reperfusion of the heart. *J Biol Chem*. 2001;276:2571–2575.

7. Hausenloy DJ, Duchen MR, Yellon DM. Inhibiting mitochondrial permeability transition pore opening at reperfusion protects against ischaemia-reperfusion injury. *Cardiovasc Res*. 2003;60:617–625.

8. Baines CP, Kaiser RA, Purcell NH, et al. Loss of cyclophilin D reveals a critical role for mitochondrial permeability transition in cell death. *Nature*. 2005;434:658–662.

9. Nakagawa T, Shimizu S, Watanabe T, et al. Cyclophilin D-dependent mitochondrial permeability transition regulates some necrotic but not apoptotic cell death. *Nature*. 2005;434:652–658.

10. Galluzzi L, Vitale I, Aaronson SA, et al. Molecular mechanisms of cell death: recommendations of the Nomenclature Committee on Cell Death 2018. *Cell Death Differ*. 2018;25:486–541.

11. Piot C, Croisille P, Staat P, et al. Effect of cyclosporine on reperfusion injury in acute myocardial infarction. *N Engl J Med*. 2008;359:473–481.

12. Cung TT, Morel O, Cayla G, et al. Cyclosporine before PCI in patients with acute myocardial infarction. *N Engl J Med*. 2015;373:1021–1031.

13. Dixon SJ, Lemberg KM, Lamprecht MR, et al. Ferroptosis: an iron-dependent form of non-apoptotic cell death. *Cell*. 2012;149:1060–1072.

14. Yang WS, SriRamaratnam R, Welsch ME, et al. Regulation of ferroptotic cancer cell death by GPX4. *Cell*. 2014;156:317–331.

15. Friedmann Angeli JP, Schneider M, Proneth B, et al. Inactivation of the ferroptosis regulator Gpx4 triggers acute renal failure in mice. *Nat Cell Biol*. 2014;16:1180–1191.

16. Fang X, Wang H, Han D, et al. Ferroptosis as a target for protection against cardiomyopathy. *Proc Natl Acad Sci U S A*. 2019;116:2672–2680.

17. Imai H, Matsuoka M, Kumagai T, Sakamoto T, Koumura T. Lipid peroxidation-dependent cell death regulated by GPx4 and ferroptosis. *Curr Top Microbiol Immunol*. 2017;403:143–170.

18. Tadokoro T, Ikeda M, Ide T, et al. Mitochondria-dependent ferroptosis plays a pivotal role in doxorubicin cardiotoxicity. *JCI Insight*. 2020;5:e132747.

19. Imai H, Hirao F, Sakamoto T, et al. Early embryonic lethality caused by targeted disruption of the mouse PHGPx gene. *Biochem Biophys Res Commun*. 2003;305:278–286.

20. Imai H, Hakkaku N, Iwamoto R, et al. Depletion of selenoprotein GPx4 in spermatocytes causes male infertility in mice. *J Biol Chem*. 2009;284:32522–32532.

21. Imai H. New strategy of functional analysis of PHGPx knockout mice model using transgenic rescue method and Cre-loxP system. *J Clin Biochem Nutr*. 2010;46:1–13.

22. Yoshida M, Minagawa S, Araya J, et al. Involvement of cigarette smoke-induced epithelial cell ferroptosis in COPD pathogenesis. *Nat Commun*. 2019;10:3145.

23. Deguchi H, Ikeda M, Ide T, et al. Roxadustat markedly reduces myocardial ischemia reperfusion injury in mice. *Circ J*. 2020;84:1028–1033.

24. Fujiwara M, Matoba T, Koga JI, et al. Nanoparticle incorporating Toll-like receptor 4 inhibitor attenuates myocardial ischaemia-reperfusion injury by inhibiting monocyte-mediated inflammation in mice. *Cardiovasc Res*. 2019;115:1244–1255.

25. Tanei T, Pradipta AR, Morimoto K, et al. Cascade reaction in human live tissue allows clinically applicable diagnosis of breast cancer morphology. *Adv Sci (Weinh)*. 2019;6:1801479.

26. Ikeda M, Ide T, Tadokoro T, et al. Excessive hypoxia-inducible factor-1α expression induces cardiac rupture via p53-dependent apoptosis after myocardial infarction. *J Am Heart Assoc*. 2021:e020895.

27. Ikeda M, Ide T, Furusawa S, et al. Heart rate reduction with ivabradine prevents cardiac rupture after myocardial infarction in mice. *Cardiovasc Drugs Ther*. 2021;36(2):257–262.

28. Ackers-Johnson M, Li PY, Holmes AP, et al. A simplified, Langendorff-free method for concomitant isolation of viable cardiac myocytes and nonmyocytes from the adult mouse heart. *Circ Res*. 2016;119:909–920.

29. Ikeda M, Ide T, Fujino T, et al. The Akt-mTOR axis is a pivotal regulator of eccentric hypertrophy during volume overload. *Sci Rep*. 2015;5:15881.

30. Ikeda M, Ide T, Fujino T, et al. Overexpression of TFAM or twinkle increases mtDNA copy number and facilitates cardioprotection associated with limited mitochondrial oxidative stress. *PLoS One*. 2015;10:e0119687.

31. Arai S, Ikeda M, Ide T, et al. Functional loss of DHRS7C induces intracellular Ca^{2+} overload and myotube enlargement in C2C12 cells via calpain activation. *Am J Physiol Cell Physiol*. 2017;312:C29–C39.

32. Inoue T, Ikeda M, Ide T, et al. Twinkle overexpression prevents cardiac rupture after myocardial infarction by alleviating impaired mitochondrial biogenesis. *Am J Physiol Heart Circ Physiol*. 2016;311(3):H509–H519.

33. Ueta T, Inoue T, Furukawa T, et al. Glutathione peroxidase 4 is required for maturation of photoreceptor cells. *J Biol Chem*. 2012;287:7675–7682.

34. Kwong JQ, Molkentin JD. Physiological and pathological roles of the mitochondrial permeability transition pore in the heart. *Cell Metab*. 2015;21:206–214.

35. Javadov S, Karmazyn M. Mitochondrial permeability transition pore opening as an end point to initiate cell death and as a putative target for cardioprotection. *Cell Physiol Biochem*. 2007;20:1–22.

36. Cui D, Arima M, Hirayama T, Ikeda E. Hypoxia-induced disruption of neural vascular barrier is mediated by the intracellular induction of Fe(II) ion. *Exp Cell Res*. 2019;379:166–171.

37. Hirayama T, Tsuboi H, Niwa M, et al. A universal fluorogenic switch for Fe(II) ion based on N-oxide chemistry permits the visualization of intracellular redox equilibrium shift toward labile iron in hypoxic tumor cells. *Chem Sci*. 2017;8:4858–4866.

38. Hirayama T, Miki A, Nagasawa H. Organelle-specific analysis of labile Fe(II) during ferroptosis by using a cocktail of various colour organelle-targeted fluorescent probes. *Metallomics*. 2019;11:111–117.

39. Kagan VE, Mao G, Qu F, et al. Oxidized arachidonic and adrenic PEs navigate cells to ferroptosis. *Nat Chem Biol*. 2017;13:81–90.

40. Ryter SW, Alam J, Choi AMK. Heme oxygenase-1/carbon monoxide: from basic science to therapeutic applications. *Physiol Rev*. 2006;86:583–650.

41. Otterbein LE, Foresti R, Motterlini R. Heme oxygenase-1 and carbon monoxide in the heart: the balancing act between danger signaling and pro-survival. *Circ Res*. 2016;118:1940–1959.

42. Yet SF, Tian R, Layne MD, et al. Cardiac-specific expression of heme oxygenase-1 protects against ischemia and reperfusion injury in transgenic mice. *Circ Res*. 2001;89:168–173.

43. Clark JE, Foresti R, Sarathchandra P, Kaur H, Green CJ, Motterlini R. Heme oxygenase-1–derived bilirubin ameliorates postischemic myocardial dysfunction. *Am J Physiol Heart Circ Physiol*. 2000;278:H643–H651.

44. Akamatsu Y, Haga M, Tyagi S, et al. Heme oxygenase-1–derived carbon monoxide protects hearts from transplant associated ischemia reperfusion injury. *FASEB J*. 2004;18:771–772.

45. Melo LG, Agrawal R, Zhang L, et al. Gene therapy strategy for long-term myocardial protection using adeno-associated virus–mediated delivery of heme oxygenase gene. *Circulation*. 2002;105:602–607.

KEY WORDS ischemia-reperfusion injury, ferroptosis, glutathione peroxidase 4, MPT-driven necrosis, cyclosporine A

APPENDIX For supplemental figures, please see the online version of this paper.